

University of New Mexico

UNM Digital Repository

Civil Engineering ETDs

Engineering ETDs

Spring 3-15-2023

ADDITIVE MANUFACTURING OF ENGINEERED CEMENTITIOUS COMPOSITES WITH ULTRA-HIGH TENSILE DUCTILITY

Amir Bakhshi

Follow this and additional works at: https://digitalrepository.unm.edu/ce_etds



Part of the [Civil Engineering Commons](#), [Construction Engineering and Management Commons](#), [Environmental Engineering Commons](#), [Other Civil and Environmental Engineering Commons](#), [Structural Engineering Commons](#), and the [Transportation Engineering Commons](#)

Recommended Citation

Bakhshi, Amir. "ADDITIVE MANUFACTURING OF ENGINEERED CEMENTITIOUS COMPOSITES WITH ULTRA-HIGH TENSILE DUCTILITY." (2023). https://digitalrepository.unm.edu/ce_etds/293

This Thesis is brought to you for free and open access by the Engineering ETDs at UNM Digital Repository. It has been accepted for inclusion in Civil Engineering ETDs by an authorized administrator of UNM Digital Repository. For more information, please contact disc@unm.edu.

Amir Bakhshi
Candidate

Department of Civil, Construction, & Environmental Engineering, University of New Mexico
Department

This thesis is approved, and it is acceptable in quality
and form for publication:

Approved by the Thesis Committee:

Prof. Dr. Maryam Hojati, Chairperson
Prof. Dr. Tang-Tat Ng
Prof. Kristina Yu

**ADDITIVE MANUFACTURING OF
ENGINEERED CEMENTITIOUS COMPOSITES
WITH ULTRA-HIGH TENSILE DUCTILITY**

BY

AMIR BAKHSHI

B.A., Architectural Engineering, IAU, Iran, 2017

M.A., Architecture, University of New Mexico, USA, 2020

MS THESIS

Submitted in Partial Fulfillment of the
Requirements for the Degree of

Master of Science

Civil Engineering

The University of New Mexico
Albuquerque, New Mexico

May, 2023

ACKNOWLEDGEMENTS

I heartily acknowledge Prof. Maryam Hojati, my advisor, for continuing to encourage me through the years of classroom teaching and the long number of months of writing and rewriting these chapters. Her guidance and professional style will remain with me as I continue my career.

I also thank my committee members, Dr. Tang-Tat Ng, and Prof. Kristina Yu, for their valuable recommendations pertaining to this study and assistance in my professional development.

ADDITIVE MANUFACTURING OF ENGINEERED CEMENTITIOUS COMPOSITES WITH ULTRA-HIGH TENSILE DUCTILITY

BY

AMIR BAKHSHI

B.A., Architectural Engineering, IAU, Iran, 2017

M.A., Architecture, University of New Mexico, USA, 2020

M.A., Civil Engineering, University of New Mexico, USA, 2023

ABSTRACT

One of the critical factors in the development of additive manufacturing in the construction industry is designing suitable materials for 3D printing applications. 3D concrete printing (3DCP) has gained significant attention due to the abundance and availability of concrete. However, concrete is a brittle material and, without proper reinforcement, cannot meet the requirements for structural purposes. Engineered Cementitious Composites (ECC), known for high ductility, and strain-hardening with low fiber contents, can potentially eliminate the need for steel reinforcement in 3D printing without any need for manual placement of reinforcement.

A set of systematic tests on ECC mix designs' fresh and hardened properties was conducted to achieve the desirable ECC for 3DCP applications. In the preliminary stage, the cement was replaced with various contents of fly ash, slag, and silica fume, in two replacement levels, 50%

and 75%. The compressive, flow table, and setting time tests were conducted to evaluate the primary mix designs. In the fresh state, the flow table test was set in a constant range of 18-20 cm to ensure the flowability of mixes.

After designing printable ECC mixes, four nominated mix designs from preliminary tests were selected to investigate the effect of ECC mix design (investigating the role of replacing cement with different supplementary cementitious materials such as fly ash, slag, metakaolin, and silica fume), fiber type (PVA vs. PE fibers) and fiber content (1.5% PVA vs. 2%PVA fibers) on the mechanical properties of 3D printed ECC components. The mechanical characterization of different mixes studied the role of mentioned parameter on compressive, tensile, and flexural strength of 3D printed ECC elements. The results indicated that ECC samples containing PE fibers could achieve ultra-high ductility with a strain capacity of over 10% with an optimized mixing procedure and viscosity modifier addition. The highest compressive strength was obtained for 50% substitution of cement by slag or fly ash. Increasing the fiber quantity from 1.5% to 2% improves the compressive strength of ECC in all cases except FA50.

TABLE OF CONTENT

LIST OF TABLES	viiiviii
LIST OF FIGURES	ix
Chapter 1	1
1. Objective and Organization	1
1.1. Introduction.....	1
1.2. Research Objectives.....	2
1.3. Research Approach	2
1.4. Outline.....	3
Chapter 2	4
2. Literature Review.....	4
2.1. Introduction to Engineered Cementitious Composites (ECC).....	4
2.1.1. What is ECC?.....	4
2.1.2. Review on mix design of ECC?.....	5
2.1.3. Fresh and hardened properties of ECC	6
2.2. Introduction to application of 3D printing in construction	7
2.2.1. What is 3D printing?.....	7
2.2.2. Fresh and hardened properties of 3D printed cementitious materials	8
2.3. Review of 3D printing of ECC	9
2.3.1. Review on mix design of printable ECC?.....	10
2.3.2. Fresh and hardened properties of 3D printed ECC materials:	10
2.3.3. Reference:	12
Chapter 3	21
3. A Preliminary Study on the Mix Design of 3D-Printable Engineered Cementitious Composite	21
3.1. Introduction.....	21
3.2. Materials and experiments	25
3.2.1. Solid materials	25
3.2.2. Mix design of ECC mixtures	26
3.2.3. Mixing Procedure and Test Methods	27
3.3. Result and discussion	29
3.3.1. Flow table result.....	30
3.3.2. Compressive test result	31
3.3.3. Setting time result	33
3.4. Conclusion	35

3.5. ACKNOWLEDGMENTS	36
3.6. REFERENCES	36
Chapter 4.....	44
4. Evaluation of Mechanical Properties of 3D-Printable Engineered Cementitious Composite.....	44
Abstract.....	44
4.1. Introduction.....	45
4.2. Methods and materials	49
4.2.1. Materials and mix designs.....	49
4.2.2. Mixing procedure.....	51
4.2.3. 3D printing setup.....	52
4.3. Test Methods.....	52
4.3.1. Compressive Strength of Cast Samples	53
4.3.2. Compressive Strength of 3D Printed Samples	54
4.3.3. Flexural strength of 3D printed samples	54
4.3.4. Uniaxial direct tensile test.....	57
4.4. Results and Discussion	59
4.4.1. Compressive test results.....	59
4.4.2. Direct tensile test.....	63
4.4.3. Flexural Test	67
4.5. Conclusions.....	73
4.6. References:.....	76
Chapter 5.....	83
5. Conclusion and Future work.....	83
5.1. Conclusion	83
5.2. Future work.....	87

LIST OF TABLES

Table 1. Chemical component of cementitious dry powders.....	Error! Bookmark not defined.
Table 2. All the ingredients are reported as a proportion by weight except PVA that is the volume percent of the total mixture.....	Error! Bookmark not defined.
Table 3. Flow table result of fresh mixtures	Error! Bookmark not defined.
Table 4. Chemical composition of mineral admixtures	Error! Bookmark not defined.
Table 5. Properties of PVA and PE fibers	Error! Bookmark not defined.
Table 6. Mix design of different ECC mixtures.....	Error! Bookmark not defined.
Table 7. Tensile properties of ECC mixes after 28 days under uniaxial direct tensile test.....	Error! Bookmark not defined.

LIST OF FIGURES

Figure 1. Failure modes of cementitious materials [2]	Error! Bookmark not defined.
Figure 2. Particle size distribution (Gradation) of River Sand.....	26
Figure 3. Compressive strength of 50% cement replacement with FA, S, and SF.	34
Figure 4. Compressive strength of 75% cement replacement with FA, S, and SF.	34
Figure 5. Setting time results of different ECC mixtures.....	35
Figure 6. Mixing procedure of ECC Mixtures	52
Figure 7. Raw materials (1), Mixer and Pump assembly (2), 3 inches diameter hose (3), 3D printer frame (4), Printing nozzle (5), 2x2 Printing bed (6), 3D printer processor (7), PC with software (8)	53
Figure 8. Primary 3D printed 150×150×60 mm sample with 20mm circular nozzle (1), four extracted 50×50×50mm cubic specimens from the primary sample (2), Compressive test setup with samples tested perpendicular to the loading direction (3).....	54
Figure 9. Three-point bending schematic test setup (1), the cross-section of the tested beam (2), primary 3D Printed slab of 100×350×50 mm with 20 mm circular nozzle (3), four extracted 140×40×40 mm beams from the primary slab (4), the third point bending test setup (5)	56
Figure 10. Uniaxial direct tensile test schematic test setup (1), dimension of dog-bone 3D printed samples (2), 3D printing the specimen inside the molds for under tension area (3), specimen showing 3D printed and cast part (4), test setup (5)	58
Figure 11. Compressive strength of specimen containing 1.5%PVA for cast and printed specimens at 28-day age (1), compressive strength of cast specimens containing 2%PVA and 2%PE for cast samples at 28 days of age (2).....	63
Figure 12. Direct tensile test strain and stress of different ECC mixes at 28-day age	66
Figure 13. Load-Displacement of ECC printed beams containing 1.5% PVA, 2% PVA and 2%PE at 28 days of age.	70
Figure 15.Relation between ultimate load and Mid-span deflection of ECC	73

Chapter 1

1. Objective and Organization

1.1. Introduction

Additive Manufacturing (AM), particularly 3D concrete printing (3DCP), has gained significant attention during the last decade. Overall, 3DCP can reduce construction costs, expand sustainable development, provide a wide range of design freedom, and resolve the need for skilled labor. However, the full potential of 3DCP cannot be realized without a suitable reinforcement approach compatible with fully automated construction. Currently, rebar reinforcement of 3D-printed structural components can fulfill the standard mechanical requirements; however, placing rebar is not fully automated, and in most cases, skilled labor is required to perform the job.

Fiber reinforcement of cementitious materials is a broadly accepted approach to improving the ductility of 3D printable cementitious materials and, on some levels, can be used as a substitution for rebar reinforcement in structural components. Engineered Cementitious Composites (ECC) are a specific class of fiber-reinforced concrete with a high ductility (i.e., up to 8% tensile strain capacity) with self-healing ability and multiple micro-cracking capacities under load with moderate fiber volume fraction (i.e., 1.5%-2%). The implication of ECC in 3D concrete printing has been investigated in several studies; nevertheless, this thesis has been carried out to investigate the possibility of designing a cost-effective ECC with locally available material in region 6.

1.2. Research Objectives

This thesis aimed to investigate the feasibility of developing ECC with locally available materials in region 6 for 3D printing applications. The first step was to develop ECC mix designs with available mineral admixtures and identify the proper proportion of each mineral admixture. Subsequently, investigating the fresh properties of each mixture with a flow table and setting time tests provided valuable insight into the printability of each ECC. The final objective was to achieve an ultra-high ductile 3D printable ECC with a strain capacity of over 8%.

1.3. Research Approach

The main objective of the first phase of the investigation was to achieve an affordable and sustainable ECC. Therefore, according to the literature review and past studies, numerous mix designs were selected. The cement was replaced with different contents of slag, silica fume, and fly ash in two replacement levels of 50% and 70%. The compressive strength and flow table test were the main criteria to evaluate each mix design suitable for 3D printing applications. The water and sand content and mixing procedure were adjusted in this phase to reach the desirable fresh properties. The second phase of the studies focused on performing mechanical tests on four nominated mix designs and improving the ductility of 3D-printed ECC. The compressive strength, tensile strength, and flexural strength of nominated mix designs with different content of PVA and PE fibers were evaluated according to ASTM standard test methods. In addition, the following test was performed on all mixtures:

- ASTM C109 / C109M: Standard Test Method for Comprehensive Strength of Hydraulic Cement Mortars
- ASTM C403: Standard Test Method for Time of Setting of Concrete Mixtures by Penetration Resistance

- ASTM C230/C230M-14: Standard Specification for Flow Table for Use in Tests of Hydraulic Cement
- ASTM C78-09: Standard Test Method for Flexural Strength of Concrete (Using Simple Beam with Third-Point Loading)
- Outlines of JSCE “Recommendations for Design and Construction of Ultra High Strength Fiber Reinforced Concrete Structures

1.4. Outline

This thesis is presented in the four remaining chapters. Chapter 2 is the literature review and current developments in ECC and 3D concrete printing. In chapter 3, a conference paper published in 2021 ASCE is presented in the preliminary study of printable ECC, numerous mix designs with a combination of different contents of fly ash, slag, and silica fume, in two replacement levels, 50%, and 75%, were developed with sufficient compressive strength to ensure the feasibility of using designed ECC in construction applications. Chapter 4 will be another journal paper, a set of four ECC mix designs with promising fresh properties suitable for 3D printing applications were developed. The ultimate goal was to achieve an ultra-high tensile 3D printable ECC with a tensile capacity of over 8%. Ultimately, a set of mechanical experiments on the effect of two types of PVA and PE fibers in two volume fractions of 1.5% and 2% have been conducted, and the results are presented in the conclusion. Finally, chapter 5 will conclude the thesis proposal with research conclusions and future work.

Chapter 2

2. Literature Review

Construction techniques have tremendously evolved through the last decade by virtue of the developments in robots allowing them to build faster using Additive Manufacturing, mainly 3D printing and also Artificial Intelligence (AI), enhancing construction safety with proper information management [1]. However, conventional construction materials, specifically concrete with brittle behavior, cannot respond to all the requirements for fully automated construction. As a result, ECC, with superior ductility and multiple microcracking, has gained significant attention as an alternative to conventional concrete for 3D printing applications. This chapter reviews two novel technologies of ECC materials and 3D printing, and finally, the application of ECC in 3D printing.

2.1. Introduction to Engineered Cementitious Composites (ECC)

Engineered Cementitious Composites (ECC) are a specific class of fiber-reinforced concrete with a high ductility (i.e., up to 8% tensile strain capacity) with self-healing ability and multiple microcracking capacities under load with moderate fiber volume fraction (i.e., 1.5%-2%) [2].

2.1.1. What is ECC?

Engineered Cementitious Composites (ECC) or Strain hardening Cement-based Composites (SHCC) is a highly Ductile Fiber Reinforced Concrete that exhibits pseudo-strain hardening,

despite the moderately low fiber volume fraction (2% and less). Figure 1 illustrates three different modes of tensile failure in cementitious materials: Brittle, quasi-brittle, and strain-hardening failure. Brittle failure can be seen in hardened cementitious materials [3]. It is described as a linear stress-strain curve with a sudden drop after the first crack (curve A). Quasi-brittle failure can be seen in most fiber-reinforced concretes. It is characterized as a linear stress-strain curve followed by a softening tail after the first crack appearance (curve B). The strain hardening failure can be observed in ECC and can be characterized as a linear stress-strain curve followed by a hardening behavior and sustaining the load after the first crack (curve C).

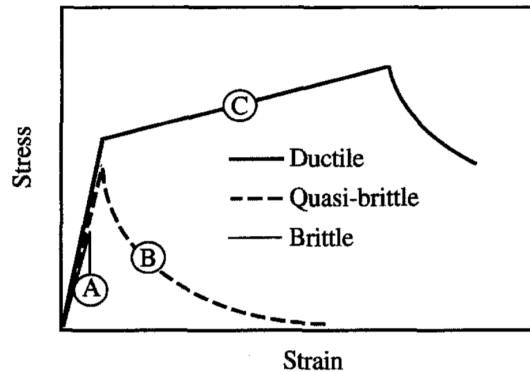


Figure 1. Failure modes of cementitious materials [3]

2.1.2. Review on mix design of ECC?

The typical ECC mixtures contain cement, fine aggregate, mineral admixtures, and short fibers. Li et al., through experimental research, discovered that fine aggregates improve the composite's elastic modulus of ECC [4]. The inclusion of mineral admixtures can affect mechanical properties of ECC. A high volume of fly ash (60%-75% of cement) in regular ECC can lower the strength and fracture toughness as it limits the pozzolanic reaction of fly ash in the matrix [5]. Zhu et.al,

discovered that the ductility of ECC can significantly improve by replacing a high volume (i.e., 50%-70%) of cement with a combination of slag and fly ash [6]. Inclusion of slag in ECC can successfully improve the compressive strength, at early age [7]. Polyvinyl alcohol (PVA) and polyethylene (PE) fibers are two specific types of fibers that are widely used in ECC. Initially, Li et al. [1] incorporated PE fibers to develop ECC, then later, Kanda and Li [35] included PVA fiber which is environmentally friendly with excellent alkali resistance for producing ECC.

2.1.3. Fresh and hardened properties of ECC

Li, in the 1990s, developed ECC in an attempt to achieve strain-hardened cementitious composites that is beyond Fiber Reinforced Concrete (FRC) tensile strength and strain capacities [8]. Due to the superior ductility of ECC, which is several hundred times that of regular concrete, ECC has been known as representative strain-hardening cementitious composites (SHCC) [9][10]. The original ECC using PE fibers exhibited compressive strength in the range of 55.7-77.2 MPa, tensile strength, and tensile strain capacity in the range of 2.9-4.8 MPa and 1.7-5.6%, respectively [11]. With the advancement in available mineral and chemical admixtures, fiber type and quantity, various mixing procedures, and production parameters, ECC can be developed based on the required structural performance. Zhou et al. improved the tensile properties and decreased the drying shrinkage by adjusting mixing sequences of freshly mixed ECC [12]. Kim et al. incorporated ground-granulated blast furnace slag in ECC to assess the influence of slag on fiber dispersion. The results demonstrated that the tensile strain capacity of Slag-ECC is approximately 50% higher than the regular ECC, most likely due to the improved fiber dispersion [13]. Li et al. developed an ECC based on the flaw size of the river sand and substituted ultrafine silica sand used for conventional ECCs, with coarse river sand, which is almost 20 times larger in terms of

particle size. The compressive strength of river sand ECC exceeded 115 Mpa, and the tensile strength and strain were more than 12 MPa and 9%, respectively [14].

2.2. Introduction to application of 3D printing in construction

Increasing productivity, providing more attractive jobs, and skilled labor shortages are all concerns that can be addressed via the prospect of automation and digitalization in construction [15]. Additive manufacturing (AM) of cementitious materials, also known as 3D concrete printing (3DCP), poses a high potential and is one of the most promising current technologies for materializing digital data to an actual product in factories and on construction sites [2,3,4]. A high degree of design freedom, automated production process, and potential for optimization are some of the significant benefits of AM in construction [19]. Aerospace, automotive, and medical industries have all examined a variety of materials integrated with 3D printing, including metal, carbon fiber, acrylonitrile butadiene styrene (ABS), aluminum, nitinol and epoxy composites [20][21][22][23][24]. In addition, the compatibility of AM with other technologies, such as machine learning and monitoring techniques, can potentially improve fabrication quality and avoid further deterioration of the part quality [25][26].

2.2.1. What is 3D printing?

Understanding the extrusion-based 3D concrete printing (3DCP) process is a significant step toward designing and optimizing 3DCP systems. Typically, there are three different categories have been defined for extrusion-based 3DCP: "i) extrusion of stiff material, similar to conventional extrusion, ii) extrusion of flowable material with or without the addition of admixture(s) in the printhead, and iii) extrusion of material using additional energy input, e.g., vibration to facilitate

delivery and deposition of stiff mixtures [16].” 3D printing has been rapidly developing in recent years as a promising technology in the construction industry that can be used to achieve environmental, economic, and other benefits. However, this layer-by-layer automated construction process is highly dependent on the availability of materials, accuracy of the printing job, cost, and production time [21].

2.2.2. Fresh and hardened properties of 3D printed cementitious materials

Concrete structures are the most common applications of robotic technologies, despite numerous challenges in the technology itself. Recent studies illustrated that future studies need to investigate the possibility of alternative construction materials and engineering designs to support 3D printing and advanced automation in construction [27]. Pumpability, extrudability, and buildability are three basic terms widely used in describing the fresh properties of cementitious materials in 3D printing [28]. Pumpability is conceived as the capability of cementitious materials to evaluate how easily the material transports from the reservoir to the nozzle [29]. Extrudability is the capability of fresh mixtures to pass from the 3D printer head through the nozzle as an intact filament without discontinuity [10,11,12]. Buildability is defined as the bearing capacity of the filament under its weight and the weight of subsequent layers after extrusion [13,14]. Several methods have investigated the integration of reinforcement with 3D-printed concrete components to improve structural performance over the past years [35]. The reinforcement method can be categorized depending on the concrete deposition time (i.e, before, during, or after deposition) and whether the reinforcement is internal or external [19]. The external reinforcement is beneficial as the printing process can be continued undisrupted, and the separately printed components can be assembled after the fact [16,17]. Another approach is considering the 3D-printed components as formwork

and installing reinforcement inside the manufactured elements. This technique can be valuable as the conventional reinforcement method can be applied by pouring regular concrete into the 3D-printed objects [38]. The alternative internal reinforcement approach is installing the reinforcement before encasing it with 3D-printed concrete. This technique might limit the height of pre-installed reinforcements [39]. The last method for internal reinforcement is during printing installation. Depositing filament layer by layer and embedding reinforcement (i.e, cable reinforcement) automatically into the concrete is a developed and tested approach [40]. Fiber reinforcement of cementitious materials is widely used as an alternative internal reinforcement. Concrete is a brittle material; adding fibers to the fresh mix before printing can improve ductility. Nonetheless, the rebar is required in most cases to meet the standards [21,22,23]. Regardless of the current developments in reinforcement methods for 3D printing purposes, there are several other methods worth considering for future studies as reinforcement techniques, such as braided lattice composites with ultra-light structures and high energy absorbent capacity [38,[45].

2.3. Review of 3D printing of ECC

Concrete is a brittle material with low tensile strength (i.e., less than 10 percent of the compressive strength). Due to the shrinkage and load bearing, the possibility of crack propagation is high [2]. Engineered cementitious composites (ECC), with superior tensile ductility, multiple cracking abilities, and strain hardening behavior, meet the requirements for sustainable infrastructures and 3D printing applications [46]. Engineered cementitious composites (ECC) resist significant tensile and shear forces and are high-performance fiber-reinforced cementitious composites (HPFRCC) [47].

2.3.1. Review on mix design of printable ECC?

Substituting ordinary Portland cement (OPC) with other supplementary cementitious materials such as fly ash, blast furnace slag, metakaolin, and silica fume is one green solution to accomplish a sustainable mix design for 3D printing applications [27,28,29]. Past studies demonstrated that the partial substitution of OPC with silica fume between 5% to 10% weight of the binder improves the fresh properties of 3D printable concrete mixture, particularly the buildability and viscosity significantly improved [42][49]. The inclusion of fly ash provides a cohesive mixture and improves pumpability. Additionally, the water demand reduces, and workability improves in most cases [51]. Adding Metakaolin (MK) can positively affect the hardened and fresh properties of 3DCP. Furthermore, MK can mitigate the drying shrinkage effect and improve the mechanical performance of cementitious mixtures due to the filling effect and its pozzolanic activity [52]. ECC typically requires an extensive mixing time (minimum of 5 min) to achieve an appropriate dispersion of fibers and other particles [46].

2.3.2. Fresh and hardened properties of 3D printed ECC materials:

The parameters used to define fresh properties of 3D printable cementitious materials (i.e., extrudability, buildability, pumpability) are also applicable for describing the fresh state of 3D printed ECC materials. Workability is another commonly used term to indirectly but quantitatively assess the rheology of cementitious materials in the fresh state. The extrudability and buildability depend on workability. High workability in freshly mixed concrete promotes extrudability, while low workability promotes buildability [53]. The workability of ECC can be evaluated using a flow table test (ASTM C1437 and ASTM C230), as used previously for analyses of thixotropic cementitious materials [53][54]. The flow table test is a convenient method that allows repeatedly evaluate freshly mixed ECC over time intervals.

The material composition and inclusion of admixtures are critical factors that significantly affect printable ECC in fresh and hardened state. The production process (cast or print) can significantly influence fiber orientation and the mechanical performance of ECC. A comparison between cast and printed ECC revealed that in-plane mechanical properties of specimens tend to be improved due to the fiber alignment in the print direction [55]. Zhou et al. discovered that strain capacity and in-plane tensile strength of printed ECC increases by 30% and 39%, respectively, by reducing the nozzle standoff distance within a specific range [56]. Hiroki et al. developed a 3D-printed ECC by incorporating 1% and 1.5% volume fractions of PE fibers with a tensile strength of 5.7 MPa and a tensile strain capacity of 3.2%. Moreover, a comparison between the cast and 3D printed samples was conducted, and due to the favorable orientation of fibers, 3D printed specimens exhibited superior strain-hardening behavior compared to the cast samples [42]. Moreover, Soltan and Li utilized 2% by volume PVA fibers to create 3D printed ECC with tensile strength and tensile strain capacity of 6 MPa and 4%, respectively [53]. Likewise, Zhu et al. developed the 3D printed ECC using PE fibers at different contents up to 2% achieved tensile strength and tensile strain capacity in the range of 5.35-5.68 MPa and 3.57-11.43% respectively [57].

2.3.3. Reference:

- [1] A. Morteza, M. Ilbeigi, and J. Schwed, “A Blockchain Information Management Framework for Construction Safety Azita,” *Comput. Civ. Eng.* 2021, pp. 811–818, 2021.
- [2] E. H. Yang, S. Wang, Y. Yang, and V. C. Li, “Fiber-bridging constitutive law of engineered cementitious composites,” *J. Adv. Concr. Technol.*, vol. 6, no. 1, pp. 181–193, 2008, doi: 10.3151/jact.6.181.
- [3] Victor C.Li, “Engineered Cementitious Composites (Ecc) – Tailored Composites through Micromechanical Modeling,” *Can. Soc. Civ. Eng.*, pp. 1–38, 1997.
- [4] V. C. Li, S. Wang, and C. Wu, “Tensile strain-hardening behavior of polyvinyl alcohol engineered cementitious composite (PVA-ECC),” *ACI Mater. J.*, vol. 98, no. 6, pp. 483–492, 2001, doi: 10.14359/10851.
- [5] H. Noorvand, G. Arce, M. Hassan, T. Rupnow, and L. N. Mohammad, “Investigation of the Mechanical Properties of Engineered Cementitious Composites with Low Fiber Content and with Crumb Rubber and High Fly Ash Content,” *Transp. Res. Rec.*, vol. 2673, no. 5, pp. 418–428, 2019, doi: 10.1177/0361198119837510.
- [6] Y. Zhu, Z. Zhang, Y. Yang, and Y. Yao, “Measurement and correlation of ductility and compressive strength for engineered cementitious composites (ECC) produced by binary and ternary systems of binder materials: Fly ash, slag, silica fume and cement,” *Constr. Build. Mater.*, vol. 68, pp. 192–198, 2014, doi: 10.1016/j.conbuildmat.2014.06.080.
- [7] Y. Zhu, Y. Yang, and Y. Yao, “Use of slag to improve mechanical properties of engineered cementitious composites (ECCs) with high volumes of fly ash,” *Constr. Build. Mater.*, vol. 36, pp. 1076–1081, 2012, doi: 10.1016/j.conbuildmat.2012.04.031.

- [8] V. C. Li, “From Micromechanics Engineering Design for Compo- of Cementitious Engineering,” *JSCE J. Struct. Mech. Earthq. Eng.*, vol. 471, no. I–24, pp. 37s–48s, 1993.
- [9] H. Ma, S. Qian, Z. Zhang, Z. Lin, and V. C. Li, “Tailoring Engineered Cementitious Composites with local ingredients,” *Constr. Build. Mater.*, vol. 101, no. Part 1, pp. 584–595, 2015, doi: 10.1016/j.conbuildmat.2015.10.146.
- [10] D. Y. Yoo and N. Banthia, “High-performance strain-hardening cementitious composites with tensile strain capacity exceeding 4%: A review,” *Cem. Concr. Compos.*, vol. 125, no. June 2021, p. 104325, 2022, doi: 10.1016/j.cemconcomp.2021.104325.
- [11] V. C. Li, D. K. Mishra, and H. C. Wu, “Matrix design for pseudo-strain-hardening fibre reinforced cementitious composites,” *Mater. Struct.*, vol. 28, pp. 586–595, 1995.
- [12] J. Zhou, S. Qian, G. Ye, O. Copuroglu, K. Van Breugel, and V. C. Li, “Improved fiber distribution and mechanical properties of engineered cementitious composites by adjusting the mixing sequence,” *Cem. Concr. Compos.*, vol. 34, no. 3, pp. 342–348, 2012, doi: 10.1016/j.cemconcomp.2011.11.019.
- [13] J. K. Kim, J. S. Kim, G. J. Ha, and Y. Y. Kim, “Tensile and fiber dispersion performance of ECC (engineered cementitious composites) produced with ground granulated blast furnace slag,” *Cem. Concr. Res.*, vol. 37, no. 7, pp. 1096–1105, 2007, doi: 10.1016/j.cemconres.2007.04.006.
- [14] Y. Li, X. Guan, C. Zhang, and T. Liu, “Development of High-Strength and High-Ductility ECC with Saturated Multiple Cracking Based on the Flaw Effect of Coarse River Sand,” *J. Mater. Civ. Eng.*, vol. 32, no. 11, pp. 1–11, 2020, doi: 10.1061/(asce)mt.1943-5533.0003405.

- [15] T. Wangler et al., “Digital Concrete: Opportunities and Challenges,” *RILEM Tech. Lett.*, vol. 1, p. 67, 2016, doi: 10.21809/rilemtechlett.2016.16.
- [16] V. Mechtcherine et al., “Extrusion-based additive manufacturing with cement-based materials – Production steps, processes, and their underlying physics: A review,” *Cem. Concr. Res.*, vol. 132, no. March, p. 106037, 2020, doi: 10.1016/j.cemconres.2020.106037.
- [17] S. Chaves Figueiredo et al., “An approach to develop printable strain hardening cementitious composites,” *Mater. Des.*, vol. 169, 2019, doi: 10.1016/j.matdes.2019.107651.
- [18] G. H. Ahmed, N. H. Askandar, and G. B. Jumaa, “A review of largescale 3DCP : Material characteristics , mix design , printing process , and reinforcement strategies,” *Structures*, vol. 43, no. July, pp. 508–532, 2022, doi: 10.1016/j.istruc.2022.06.068.
- [19] A. Paolini, S. Kollmannsberger, and E. Rank, “Additive manufacturing in construction: A review on processes, applications, and digital planning methods,” *Addit. Manuf.*, vol. 30, no. October, p. 100894, 2019, doi: 10.1016/j.addma.2019.100894.
- [20] A. Haleem and M. Javaid, “3D printed medical parts with different materials using additive manufacturing,” *Clin. Epidemiol. Glob. Heal.*, vol. 8, no. 1, pp. 215–223, 2020, doi: 10.1016/j.cegh.2019.08.002.
- [21] P. Wu, J. Wang, and X. Wang, “A critical review of the use of 3-D printing in the construction industry,” *Autom. Constr.*, vol. 68, pp. 21–31, 2016, doi: 10.1016/j.autcon.2016.04.005.
- [22] S. M. Saleh Mousavi-Bafrouyi, R. Eslami-Farsani, and A. Geranmayeh, “Effect of stacking sequence on the mechanical properties of pseudo-ductile thin-ply unidirectional carbon-basalt

fibers/epoxy composites,” *J. Ind. Text.*, vol. 51, no. 2, pp. 2835S-2852S, 2022, doi: 10.1177/1528083720978400.

[23] S. M. Saleh Mousavi-Bafrouyi, R. Eslami-Farsani, and A. Geranmayeh, “The Temperature Effects on the Mechanical Properties of Pseudo-ductile Thin-ply Unidirectional Carbon-basalt Fibers/Epoxy Hybrid Composites with Different Stacking Sequences,” *Fibers Polym.*, vol. 22, no. 11, pp. 3162–3171, 2021, doi: 10.1007/s12221-021-1052-4.

[24] S. Behseresht and M. Mehdizadeh, “Mode I&II SIFs for semi-elliptical crack in a cylinder wrapped with a composite layer,” 1399, [Online]. Available: <https://civilica.com/doc/1029087>.

[25] J. Lyu, J. Akhavan, and S. Manoochehri, “Image-based dataset of artifact surfaces fabricated by additive manufacturing with applications in machine learning,” *Data Br.*, vol. 41, p. 107852, 2022, doi: <https://doi.org/10.1016/j.dib.2022.107852>.

[26] J. Lyu, J. Akhavan Taheri Boroujeni, and S. Manoochehri, “In-Situ Laser-Based Process Monitoring and In-Plane Surface Anomaly Identification for Additive Manufacturing Using Point Cloud and Machine Learning.” Aug. 17, 2021, doi: 10.1115/DETC2021-69436.

[27] M. Gharbia, A. Chang-Richards, Y. Lu, R. Y. Zhong, and H. Li, “Robotic technologies for on-site building construction: A systematic review,” *J. Build. Eng.*, vol. 32, no. April, p. 101584, 2020, doi: 10.1016/j.jobbe.2020.101584.

[28] Z. Li et al., “Fresh and hardened properties of extrusion-based 3D-printed cementitious materials: A review,” *Sustain.*, vol. 12, no. 14, pp. 1–33, 2020, doi: 10.3390/su12145628.

- [29] M. Amran et al., “3D-printable alkali-activated concretes for building applications: A critical review,” *Constr. Build. Mater.*, vol. 319, no. November 2021, p. 126126, 2022, doi: 10.1016/j.conbuildmat.2021.126126.
- [30] S. Lim, R. A. Buswell, T. T. Le, S. A. Austin, A. G. F. Gibb, and T. Thorpe, “Developments in construction-scale additive manufacturing processes,” *Autom. Constr.*, vol. 21, no. 1, pp. 262–268, 2012, doi: 10.1016/j.autcon.2011.06.010.
- [31] T. T. Le, S. A. Austin, S. Lim, R. A. Buswell, A. G. F. Gibb, and T. Thorpe, “Mix design and fresh properties for high-performance printing concrete,” *Mater. Struct. Constr.*, vol. 45, no. 8, pp. 1221–1232, 2012, doi: 10.1617/s11527-012-9828-z.
- [32] Z. Malaeb, H. Hachem, A. Tourbah, T. Maalouf, N. El Zarwi, and F. Hamzeh, “3D Concrete Printing: Machine and Mix Design,” *Int. J. Civ. Eng. Technol.*, vol. 6, no. April, pp. 14–22, 2015, [Online]. Available: http://www.researchgate.net/profile/Farook_Hamzeh/publication/280488795_3D_Concrete_Printing_Machine_and_Mix_Design/links/55b608c308aec0e5f436d4a1.pdf.
- [33] V. Saruhan, M. Keskinateş, and B. Felekoğlu, “A comprehensive review on fresh state rheological properties of extrusion mortars designed for 3D printing applications,” *Constr. Build. Mater.*, vol. 337, no. April, 2022, doi: 10.1016/j.conbuildmat.2022.127629.
- [34] G. W. Ma, L. Wang, and Y. Ju, “State-of-the-art of 3D printing technology of cementitious material—An emerging technique for construction,” *Sci. China Technol. Sci.*, vol. 61, no. 4, pp. 475–495, 2018, doi: 10.1007/s11431-016-9077-7.

- [35] D. Asprone, C. Menna, F. P. Bos, T. A. M. Salet, J. Mata-Falcón, and W. Kaufmann, “Rethinking reinforcement for digital fabrication with concrete,” *Cem. Concr. Res.*, vol. 112, no. January, pp. 111–121, 2018, doi: 10.1016/j.cemconres.2018.05.020.
- [36] D. Asprone, F. Auricchio, C. Menna, and V. Mercuri, “3D printing of reinforced concrete elements: Technology and design approach,” *Constr. Build. Mater.*, vol. 165, pp. 218–231, 2018, doi: 10.1016/j.conbuildmat.2018.01.018.
- [37] T. A. M. Salet, Z. Y. Ahmed, F. P. Bos, and H. L. M. Laagland, “Design of a 3D printed concrete bridge by testing*,” *Virtual Phys. Prototyp.*, vol. 13, no. 3, pp. 222–236, 2018, doi: 10.1080/17452759.2018.1476064.
- [38] J. Teizer, A. Blickle, T. King, O. Leitzbach, and D. Guenther, “Large scale 3D printing of complex geometric shapes in construction,” *ISARC 2016 - 33rd Int. Symp. Autom. Robot. Constr.*, vol. i, no. Isarc, pp. 948–956, 2016, doi: 10.22260/isarc2016/0114.
- [39] E. Lloret et al., “Complex concrete structures: Merging existing casting techniques with digital fabrication,” *CAD Comput. Aided Des.*, vol. 60, pp. 40–49, 2015, doi: 10.1016/j.cad.2014.02.011.
- [40] F. P. Bos, Z. Y. Ahmed, E. R. Jutinov, and T. A. M. Salet, “Experimental exploration of metal cable as reinforcement in 3D printed concrete,” *Materials (Basel)*, vol. 10, no. 11, 2017, doi: 10.3390/ma10111314.
- [41] B. Zhu, J. Pan, Z. Zhou, and J. Cai, “Mechanical properties of engineered cementitious composites beams fabricated by extrusion-based 3D printing,” *Eng. Struct.*, vol. 238, no. October 2020, p. 112201, 2021, doi: 10.1016/j.engstruct.2021.112201.

- [42] H. Ogura, V. N. Nerella, and V. Mechtcherine, “Developing and testing of Strain-Hardening Cement-Based Composites (SHCC) in the context of 3D-printing,” *Materials (Basel)*, vol. 11, no. 8, pp. 1–18, 2018, doi: 10.3390/ma11081375.
- [43] T. T. Le et al., “Mix design and fresh properties for high-performance printing concrete,” *Mater. Struct. Constr.*, vol. 45, no. 8, pp. 1221–1232, 2012, doi: 10.1617/s11527-012-9828-z.
- [44] M. M. Abedi, R. Jafari Nedoushan, M. Sheikhzadeh, and W. R. Yu, “The crashworthiness performance of thin-walled ultralight braided lattice composite columns: Experimental and finite element study,” *Compos. Part B Eng.*, vol. 202, no. June, p. 108413, 2020, doi: 10.1016/j.compositesb.2020.108413.
- [45] M. M. Abedi, R. Jafari Nedoushan, and W. R. Yu, “Enhanced compressive and energy absorption properties of braided lattice and polyurethane foam hybrid composites,” *Int. J. Mech. Sci.*, vol. 207, no. June, p. 106627, 2021, doi: 10.1016/j.ijmecsci.2021.106627.
- [46] V. C. Li et al., “On the emergence of 3D printable Engineered, Strain Hardening Cementitious Composites (ECC/SHCC),” *Cem. Concr. Res.*, vol. 132, no. April, p. 106038, 2020, doi: 10.1016/j.cemconres.2020.106038.
- [47] M. D. Lepech and V. C. Li, “Large-scale processing of engineered cementitious composites,” *ACI Mater. J.*, vol. 105, no. 4, pp. 358–366, 2008, doi: 10.14359/19897.
- [48] J. Teixeira, C. O. Schaefer, L. Maia, B. Rangel, R. Neto, and J. L. Alves, “Influence of Supplementary Cementitious Materials on Fresh Properties of 3D Printable Materials,” *Sustain.*, vol. 14, no. 7, pp. 1–9, 2022, doi: 10.3390/su14073970.

- [49] A. Kazemian, X. Yuan, E. Cochran, and B. Khoshnevis, “Cementitious materials for construction-scale 3D printing: Laboratory testing of fresh printing mixture,” *Constr. Build. Mater.*, vol. 145, pp. 639–647, 2017, doi: 10.1016/j.conbuildmat.2017.04.015.
- [50] Z. Xu, D. Zhang, H. Li, X. Sun, K. Zhao, and Y. Wang, “Effect of FA and GGBFS on compressive strength, rheology, and printing properties of cement-based 3D printing material,” *Constr. Build. Mater.*, vol. 339, p. 127685, 2022, doi: <https://doi.org/10.1016/j.conbuildmat.2022.127685>.
- [51] M. D. A. Thomas, “Optimizing the Use of Fly Ash in Concrete,” *Portl. Cem. Assoc.*, p. 24, 2007.
- [52] Z. Duan, L. Li, Q. Yao, S. Zou, A. Singh, and H. Yang, “Effect of metakaolin on the fresh and hardened properties of 3D printed cementitious composite,” *Constr. Build. Mater.*, vol. 350, no. August, p. 128808, 2022, doi: 10.1016/j.conbuildmat.2022.128808.
- [53] D. G. Soltan and V. C. Li, “A self-reinforced cementitious composite for building-scale 3D printing,” *Cem. Concr. Compos.*, vol. 90, pp. 1–13, 2018, doi: 10.1016/j.cemconcomp.2018.03.017.
- [54] Z. Quanji, “Thixotropic behavior of cement-based materials : effect of clay and cement types,” p. 126, 2010.
- [55] J. Yu and C. K. Y. Leung, “Impact of 3D printing direction on mechanical performance of strain-hardening cementitious composite (SHCC),” in *RILEM Bookseries*, vol. 19, 2019, pp. 255–265.

[56] W. Zhou, Y. Zhang, L. Ma, and V. C. Li, “Influence of printing parameters on 3D printing engineered cementitious composites (3DP-ECC),” *Cem. Concr. Compos.*, vol. 130, no. January, p. 104562, 2022, doi: 10.1016/j.cemconcomp.2022.104562.

[57] B. Zhu, J. Pan, B. Nematollahi, Z. Zhou, Y. Zhang, and J. Sanjayan, “Development of 3D printable engineered cementitious composites with ultra-high tensile ductility for digital construction,” *Mater. Des.*, vol. 181, no. July, p. 108088, 2019, doi: 10.1016/j.matdes.2019.108088.

Chapter 3

3. A Preliminary Study on the Mix Design of 3D-Printable Engineered Cementitious Composite

ABSTRACT

One of the challenges in applying 3D-printing in the construction industry is the concrete mix design. This paper is a preliminary study on the design of a printable Engineered Cementitious Composite (ECC). The cement was replaced with a combination of different contents of fly ash, slag, and silica fume, in two replacement levels, 50%, and 75%, and their compressive strength and setting time were evaluated. To assure the flowability of the mixtures, the flow table results were set in a constant range of 19-20 cm. The results indicate that 50% cement-substitution by slag/fly ash resulted in the largest strength. The incorporation of slag shortened the setting time and improved the strength of ECC mixtures. The cement substitution by fly ash lowered the water demand, enhanced workability, and up to 50% cement replacement improved the compressive strength. The addition of 10% silica fume reduced compressive strength and extended the setting time.

3.1. Introduction

Additive manufacturing (AM), also known as 3D-printing, of cementitious materials has a high capacity to develop automation in the construction industry [1]. There are some challenges in applying AM in the 3D-printing of concrete materials, limiting the broad application of these innovative techniques in the construction industry. Incorporation of reinforcing components, cold joint formation between layers, durability, and fresh properties of cementitious mixtures are some of the challenges. Over the last few years, some of these engineering challenges, specifically the

fresh characteristics of cementitious mixtures and processing parameters, have been studied and addressed in numerous technical papers (Soltan and Li 2018, Roussel 2018, Roussel et al. 2020, Albar et al. 2020, Kazemian et al. 2017, Perrot et al. 2012, Weng et al. 2019, Wolfs et al. 2018). The previous research showed that novel 3D-printing technique must be engineered and customized according to the fresh property requirements [8]

Concrete is a brittle material and possesses a low tensile strength (i.e., less than 10 percent of compressive strength), which causes the occurrence and propagation of cracks due to load or changing environmental conditions [9]. While the evolution of concrete strength, durability performance, and material greenness each address a particular need, adopting a comprehensive approach is crucial. Engineered Cementitious Composites (ECC) are a novel class of high-performance fiber-reinforced cementitious composites designed and optimized to exhibit a high tensile ductility [10]. The emergence of ECC presented a comprehensive solution that possesses characteristics that support infrastructure resilience, durability, sustainability and, reduction of operations and maintenance needs simultaneously [9].

ECC materials are known for outstanding properties, such as high ductility varied from 3-7%, tight crack width around 60 μ m, and the low fiber content of 1% to 2% volume fraction [11]. The reason to categorize the ECC as a strain-hardening material is a similarity between ECC and metal performances when subjected to external loads. The ECC specimens continue to bear the load after the emergence of the first crack resulting from the interaction between the fiber and matrix (Li 1992 and Yang et al. 2008). Furthermore, the compressive strength of ECCs also has a vital role in the capability of cementitious matters, especially for the structural elements, to sustain the human-induced load during their service life. Ranade [14] emphasized in his research study the existence of a balance between the compressive strength and tensile strength to achieve a high

strength composite (HSC) and high ductility concrete (HDC) simultaneously. Different compressive strength values have been reported up to now for ECC, which are ranged from 10 MPa (designed for water fire-proofing) [15], to 200 MPa (High Strength ECC) [14].

For the 3D-printing of civil infrastructure, the implementation of fiber-reinforced ECC can yield significant benefits such as an enhanced structural capacity, durability, and resiliency. As such, ECC's unique mechanical properties place this novel composite as an excellent candidate for the 3D-printing of concrete structures. While ECC is a promising material for 3D-printing implementation, several challenges still exist for its successful implementation [16][17]. To retain the ECC's strain-hardening property, high fiber content (~2% by volume) and small fiber diameter (typically below 50 μm) are essential, leading to a paradoxical demand between pumpability and buildability [18].

Four crucial terms widely used in the determination of fresh properties of cementitious materials in the 3D-printing include flowability, extrudability, buildability, and open time [19]. The flowability is defined as flow behavior of fresh material in pumping system that guarantees the easy transportation of cement paste during pumping [20]. The extrudability is the capability of fresh cement paste to pass through the nozzle as a continuous and intact filament [21] [22][23]. In addition, the buildability can be introduced as the bearing load capacity of printed filament to sustain their weight and weight of subsequent layers (Lim et al. 2012; [24]; [2]. It should be noted that the open time is defines as elapsed between the initial contact of dry mix and water and the time when the material is printable (flowable in the pumping system and extrudable in the printing [19]. Previous research showed that a value between 19-25 cm for the flow table test in the first hour provides good flowability for the fresh concrete to pump and extrude 3D-printing concrete ink [25].

One of the green solutions to make concrete mixtures a more sustainable material is to substitute ordinary Portland cement (OPC) partially with supplementary cementitious materials such as fly ash, different types of slags (copper slag, steel slag), silica fume, and metakaolin. Previous studies[26]–[28] showed the effect of incorporating these mineral admixtures in ECC's fresh and hardened properties and accordingly, the printability characteristics of this material. It was indicated that the inclusion of silica fume between 5% to 10% weight of binder improves buildability and viscosity of the fresh 3D-printed mixture [29], [30]. The optimum amount of silica fume can improve flowability and cohesiveness of mixture beyond which further addition of silica fume would cause a reduction in strength [31]. Nano-clay (NC) has a considerable impact on cohesion and thixotropy of mixture and enhances the shape stability of the fresh 3D-printed mixture [2], [32], [33]. A high content of NC exhibits low cohesion resulting in discontinuities in printing ink; on the other hand, the inclusion of 1 mass% NC enhances the compressive strength of specimen around 23 MPa in one day [34]. Due to the spherical shape of the fly ash particles, the flowability of mixtures would improve; additionally, a lower surface area to volume ratio reduces water demand [35]. It was shown that the high content of fly ash on ECC reduced the crack width due to the high interface frictional bond that restrains the slippage of fibers [36]. Moreover, it was indicated that replacing cement with a high volume of fly ash (62% and 75% cement replacement with fly ash) resulted in tensile strength reduction but an increase in tensile ductility of ECC composites [37].

This paper is a preliminary phase of a Tran Set project to investigate the feasibility of using available materials from the local suppliers in region 6 for producing an extrudable ECC mixture. The main objective of this phase is to design ECC mixtures with sufficient compressive strength and fresh properties that can be used in 3D-printing application. The compressive strength of

designed mixtures was evaluated at 7-day and 14-day ages. Additionally, to ensure the mixtures' flowability, in this phase of the project, the amount of water for the designed mixtures was set to lead to flowable mixtures with similar flow table test results (i.e., 19-20 cm). The outputs from this preliminary phase will prepare the ground for the next stages of this project. In the next phases, we will examine the compressive strength of designed ECC in later ages, the tensile strength and ductility, extrudability, buildability, and hardened properties of 3D-printed ECC components.

3.2. Materials and experiments

3.2.1. Solid materials

The primary objective of this study is to design a printable ECC with available materials from the local suppliers in region 6. To achieve this goal, we tried to contact the local and prepare the required admixtures and materials for this study. The mineral/chemical admixtures and other constituents of ECC mixtures include (1) Type I/II Ordinary Portland Cement (C), (2) Type-F Fly Ash (FA), (3) River Sand (RS) with fineness modulus of 2.3 and a maximum size of 3.36, (4) High Range Water Reducer (HRWR), (5) Silica Fume (SF), (6) Iron Blast Furnace Slag (S), (7) non-oil coated RECS15 polyvinyl alcohol PVA fibers. Table 1 presents the chemical compositions of solid materials. The aggregate used in this study was a natural river-sand with a bulk dry specific gravity of 2.59 and absorption capacity of 0.44%. Figure 1 displays the gradation curve of RS.

Table 1. Chemical component of cementitious dry powders

Material	SiO ₂	Al ₂ O ₃	Fe ₂ O ₃	CaO	MgO	SO ₃	K ₂ O	TiO ₂	Na ₂ O	Specific Gravity
Cement (C)	19.24	4.75	3.35	65.8	2.20	3.61	0.54	0.21	-	3.13
Slag (S)	30.8	11.45	2.26	47.5	3.65	3.03	0.38	-	0.17	2.91
Silica fume (SF)	97.8	-	-	-	-	0.3	-	-	0.01	2.2
Fly Ash (FA.)	61.27	23.18	5.09	2.11	1.19	0.30	1.43	-	1.44	2.09

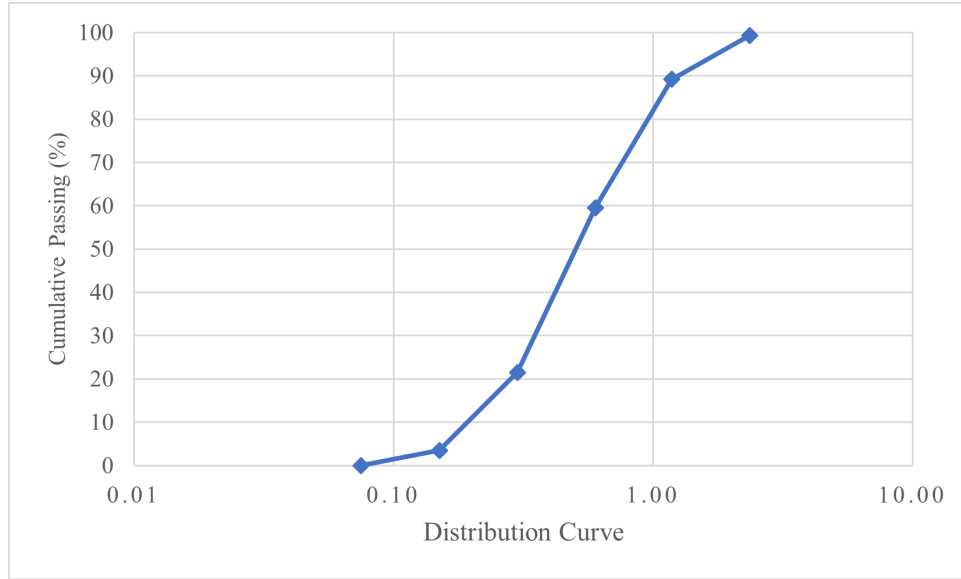


Figure 1. Particle size distribution (Gradation) of River Sand

3.2.2. Mix design of ECC mixtures

Nine ECC mixtures were designed and tested in this study (Table 2). The mixtures were labeled as FA50 (representing a hybrid binder of 50%(wt) FA and 50%(wt) C); S50 (representing a hybrid binder of 50%(wt) S and 50%(wt) C), FA75 (representing a hybrid binder of 75%(wt) FA and 25%(wt) C), S75 (demonstrating a hybrid binder of 75%(wt) S and 25%(wt) C), FA40-SF10 (representing a hybrid binder of 40%(wt) FA, 10%(wt) SF and 50%(wt) C), FA65-SF10 (representing a hybrid binder of 65%(wt) FA, 10%(wt) SF and 25%(wt) C), FA50-S25 (representing a hybrid binder of 50%(wt) FA, 25%(wt) S and 25%(wt) C), FA25-S50 (representing a hybrid binder of 25%(wt) FA, 50%(wt) S and 25%(wt) C), FA40-S25-SF10 (representing a hybrid binder of 40%(wt) FA, 25%(wt) S, 10% (wt) SF and 25%(wt) C).

In the light of the flow-characteristic influence on the printability of the fresh ECC mixtures, in this research, the attempt was made to develop different ECC mixtures by fixing the flow table of fresh mixtures in the range 19-20 cm. For all mixtures, the Water to Binder (including a combination of C, FA, S, and SF) ratio, (W/B)_{wt}, was maintained at 0.27; the quantity of HRWR

was 150 ml per 100 kg of the cementitious binder. After mixing the materials, the flow table test was conducted, and the amount of water for each mixture was adjusted (water was either added or removed) to achieve 19-20 cm flow table test results.

Table 2. All the ingredients are reported as a proportion by weight except PVA that is the volume percent of the total mixture.

#	Mix ID	C/B	FA/B	S/B	SF/B	W/B	RS/B	HRWR (%) ¹	Fibers (Vol%)	Adjusted W/B
1	FA50	0.50	0.50	0.00	0.00	0.27	0.25	0.002	1.50	0.26
2	FA75	0.25	0.75	0.00	0.00	0.27	0.25	0.004	1.50	0.24
3	S50	0.50	0.00	0.50	0.00	0.27	0.25	0.002	1.50	0.33
4	S75	0.25	0.00	0.75	0.00	0.27	0.25	0.004	1.50	0.32
5	FA40-SF10	0.50	0.40	0.00	0.10	0.27	0.25	0.003	1.50	0.33
6	FA65-SF10	0.25	0.65	0.00	0.10	0.27	0.25	0.006	1.50	0.29
7	FA50-S25	0.25	0.50	0.25	0.00	0.27	0.25	0.006	1.50	0.26
8	FA25-S50	0.25	0.25	0.50	0.00	0.27	0.25	0.006	1.50	0.29
9	FA40-S25-SF10	0.25	0.40	0.25	0.10	0.27	0.25	0.006	1.50	0.31

Note: 1. %HRWR dosage by weight of Binder

2. C: Cement; FA: Fly Ash; S: Slag; SF: Silica Fume; W: Water; RS: River Sand; B: Binder; HRWR: High Range Water Reducer

3. all ratios are weight (wt) ratio but the volumetric fiber content.

3.2.3. Mixing Procedure and Test Methods

To ensure consistency of the mixture, preparation and mixing of the ECC mortars followed a specific procedure. All mortars were mixed following ASTM C305-14. Dry powders, i.e., cement, fly ash, slag, silica fume, and river sand) were dry-mixed in advance and consistently for 15 min at slow speed (140±5 RPM) in a Hobart mixer. HRWR dissolved in water, then added to the dry powders slowly and mixed with them for another 5 minutes. Finally, PVA fibers were added to the mixture and blended with other ingredients for 10 minutes in medium speed (285±10 RPM).

The baseline of this study is checking the mechanical and fresh properties of the ECC mixtures based on their flowability. For evaluating the mechanical properties of designed ECCs, the characteristics such as compressive strength, flowability, and setting time were assessed. This

procedure paved the way to reach a mix-design appropriate for 3D-printing. The details of how the tests were performed are presented in this section.

3.2.3.1. Compressive test

The compressive strength of the designed ECCs indicates the suitability of these materials for structural applications. Therefore, it is worthy of studying the viability of prepared mixtures by assessing their compressive strength. To measure the compressive strength of mixtures, the fresh mortar was cast in two layers of $50 \times 50 \times 50$ mm cube molds immediately after mixing according to ASTM C109-20. Each layer of mortar was compacted 25 times with a rod. The samples were demolded at 24 hours and then moist cured (100% RH, $23 \pm 0.5^\circ\text{C}$) until the testing day. The cubes were tested after 7 and 14 days at a loading rate of 0.25 MPa/s.

3.2.3.2. Flow Table Test

The fresh behavior of cementitious materials plays an essential role in the flowability and extrudability of the mixtures for the 3D-printing. The more flowable the cementitious mixture, the easier movement and extrusion of fresh mortar occur in the hose/extruder for the 3D-printing process. The flowability of the specimens was evaluated according to ASTM C1437. In this test, after placing the conical mold (70mm top diameter by 100mm bottom diameter in 50mm height) at the center of standard flow table, one layer of mortar about 25mm of thickness was added into the mold and tamped 20 times. Subsequently, the mold was filled with the second layer and tamped 20 times. To make a plane surface even surface, the extra mortar was removed. The cone-shape mold was lifted and system of top table and remained mortar is shaken by dropping the table 25 times per 15s. The diameter of mortar on the table surface should be recorded just before and after the table dropping. The flow table results of different mixtures were kept constant between 19-20 mm by adjusting the W/B ratio to have a flowable mortar for the printing process.

3.2.3.3. Setting time test

The initial setting time defined as the time elapsed from the first contact of dry mix powder with water until paste is stiffen enough to reach a penetration resistance of 3.5MPa. (ASTM C125-15b)

Open time is a new term that is mostly used for the 3D-printing, and it is defined as the time elapsed between the instant of adding water until the time that fresh paste is printable[38]. Previous studies (Kazemian et al. 2017, Panda et al. 2019) indicated that the open time of printable concrete is always before the initial setting time. While there is no direct relation between setting time and open time for printable concrete, it can be assumed that the longer initial setting time results in a longer open time. In this study, we are using this test method as an indirect indicator for the open time. The convenient test method that gives the researcher the progress of structuration over time is the Vicat needle test (i.e., ASTM C1941). To perform this test method, the fresh cement paste is molded in a container (measuring 70mm top opening diameter by 80mm bottom opening diameter in 40mm height), and a periodic test is done to outline the setting status. In this test a straight steel needle is used to penetrate the cement paste in the mold. The penetration shows the trend of setting procedure; the more is the needle penetration, the lower is the stiffness of cement paste. The penetration is a way to indicate the initial setting time, the time at which the Vicat test is continued until penetration value reaches 25mm. Before this point, due to the softness of the cement paste, the penetration depth is greater. The final setting time, according to this method, is time elapsed from the first contact of water and dry ingredient and time at which the 1-mm needle does not leave any complete circular impression on the surface of cement paste. For the final setting time, two additional points on different sides of the cement paste were tested.

3.3. Result and discussion

This paper is the primary study on the design of ECC mixtures to achieve a 3D-printable material for construction. For this paper, we started our investigation by measuring the compressive

strength, setting time, and flow table of fresh mixtures to evaluate the role of different combinations of admixtures on the mechanical and fresh properties of the ECCs. The results of this study were used to identify admixtures that can produce structurally viable ECC mixtures (i.e., mixtures with adequate workability (19-20 flow table result) and compressive strength > 40 MPa). The results of different tests are presented in this section separately.

3.3.1. Flow table result

Since designed ECC mixtures exhibited different water demands in their fresh stage, and to keep them all flowable and buildable for the 3D-printing phase, we decided to adjust the water to binder ratio according to the flow table results in this preliminary stage of the study. Table 3 displays the amount of flow table test results of different mixtures.

Table 3. Flow table result of fresh mixtures

#	Mix ID	Flow Table (mm)	Initial W/B	Adjusted W/B
1	FA50	20	0.27	0.26
2	FA75	20	0.27	0.24
3	S50	19.8	0.27	0.33
4	S75	19.9	0.27	0.32
5	FA40-SF10	19	0.27	0.33
6	FA65-SF10	20	0.27	0.29
7	FA50-S25	20	0.27	0.26
8	FA25-S50	20	0.27	0.29
9	FA40-S25-SF10	19.9	0.27	0.31

The amount of adjusted water to binder (W/B) ratio in Table 3 indicates that the fly ash-rich ECC mixtures led to a lower adjusted W/B ratio (i.e., 0.24) than those of other mixtures. It is likely because of the spherical shape of fly ash particles that making them act as a lubricant in the fresh ECC mixtures; thus, they need a lower amount of water to reach a specific flow. In contrast, the

ECC mixtures contain a large slag; they need more water to reach a 19-20 cm flow table (i.e., adjusted W/B=0.33).

3.3.2. Compressive test result

The compressive strength of the designed ECC mixtures was measured in two ages (i.e., 7-day and 14-day). As displayed in Table 1, two levels of cement substitution (i.e., 50%(wt) and 75%(wt), where their C/B wt ratios are 0.50 and 0.25, respectively) by other mineral admixtures (i.e., FA, S, and SF) were studied in this paper. The compressive strength of ECC mixtures at 50% and 75% cement-replacement levels are shown in Figures 2 and 3, respectively. Each data set for compressive strength at 7 and 14 days is the average of three test results, along with standard deviation. Dark blue columns represent the strength at 7 days, and light blue ones are the compressive strength of ECCs at 14 days. In general, replacing 50%(wt) cement with other mineral admixtures (Figure 2) led to the highest compressive strength in comparison to 75%(wt) replacement level (Figure 3). This would show the role of cement on strength gain of concrete mixtures. Additionally, it is noticeable that replacing cement with slag at both substitution levels improved the compressive strength of ECC mixtures compared to fly ash ones. The 14-day strength of S50 mortar was 64 MPa (50% cement replacement), which is the highest strength achieved among all mixtures tested (approximately 17% greater than the corresponding strength of the FA50 mortar, 23% higher than the 14-day strength of S75, and twice of the compressive strength of FA75 at 14 days). These results are in agreement with other studies (Richardson 2006, Lee et al. 2015, Kim et al. 2007) that also showed that strength improved with a larger amount of calcium because of higher slag content, and as such greater calcium dissolution and precipitation of C-S-H gel. Accordingly, in terms of compressive strength of ECCs, and among the utilized admixtures (i.e., FA, SF, and S), slag could be a great sustainable replacement for cement. However, to make sure

the materials are sufficient to be used in constructing structures, we need to perform more mechanical tests, particularly the tensile strength and ductility, which are the essential features of ECC compared to conventional concrete mixtures.

Fly ash particles have a smooth spherical shape; therefore, they act as a lubricant in the fresh concrete mixtures, lead to a lower W/B ratio (check Table 2 and 3) and improve the concrete mechanical properties up to some level. Additionally, it should be noted that the presence of fly ash in ECC could reduce the interfacial bond strength of matrix and fiber [36] and enhances the dispersion of the fibers in the fresh mixture. On the other hand, for high fly ash content (such as FA75) in the ECC mixture, the small fly ash particles could act as the filler; thus, two adjacent particles would freely slide on each other and lower the interlocking and load transition capability of the mixture.

Kwan and Li (2013) also reported that replacing cement with a lower amount of fly ash increases the packing density of ECC mixtures that would improve the strength and durability of the hardened mixtures. As it is shown in Figures 2 and 3, replacement of cement with fly ash up to some level (i.e., FA50%) improved the compressive strength since the adjusted W/B ratio was low compared to other mixtures; while a larger cement substitution by fly ash (FA75) decreased the 14-day compressive strength by 43%. A similar phenomenon was observed after adding silica fume to ECC mixtures. Silica fume by itself could also act as a filler and densify the hardened matrix, but together with a high amount of spherical fly ash particles, it would increase the possibility of sliding of two adjacent particles in the cement paste. As such, replacement 10% of fly with the silica fume in FA50 resulted in FA40-SF10, and according to the results of Figure 2, this substitution led to 17% reduction of compressive strength. The same trend was observed for the 75% replacement level in Figure 3. Therefore, based on the trends observed for 50% and 75%

replacement, the addition of 10% silica fume negatively impacts the compressive strength. Still, more mechanical tests, including tensile strength and ductility, should be performed to finalize the effect of different admixtures on designing viable ECC mixtures for 3D-printing. Additionally, according to the previous research (Ogura et al. 2018; Zhu et al. 2014), silica fume would improve the buildability of fresh concrete mixtures for 3D-printing and keeping this admixture would be beneficial at some point. This study is primary research that will not end in any conclusion about printable ECC mixtures' design. In the next phases of this research, the 28-day compressive strength and tensile strength of dog bone specimens will be evaluated, and finally, the extrudability and buildability of the mixtures will be examined.

3.3.3. Setting time result

Figure 4 displays the initial and final setting times of different ECC mortars. Among all of the designed mixtures, the mixtures which contain 10% silica fume (i.e., FA65-SF10, FA40-SF10, and FA40-S25-SF10) exhibited the longest setting time. Accordingly, the incorporation of 10% silica fume would extend the setting and hardening process of ECC mixtures, resulting in a longer open time. In contrast, the slag-rich ECC mixture (S75) showed the shortest setting time compared to the other ECC mixtures, likely due to a greater C-S-H gel formation. Higher slag content may lead to a larger amount of dissolved calcium being released by slag dissolution. Thus, more C-S-H gel would form and be incorporated into the matrix to accelerate the hardening process (Roussel et al. 2012, (Roussel et al. 2012, Lee et al. 2015, Norrarat et al. 2019, Richardson 2006). Further research is required to explain these observations more accurately. Setting time would help arrange the 3D-printing process and extrude the fresh material continuously before it gets hard.

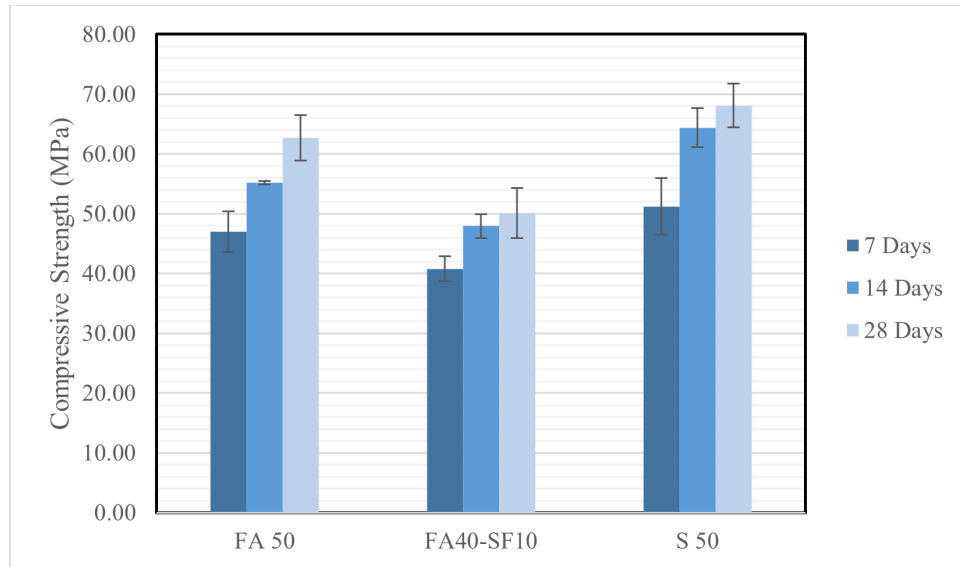


Figure 2. Compressive strength of 50% cement replacement with FA, S, and SF.

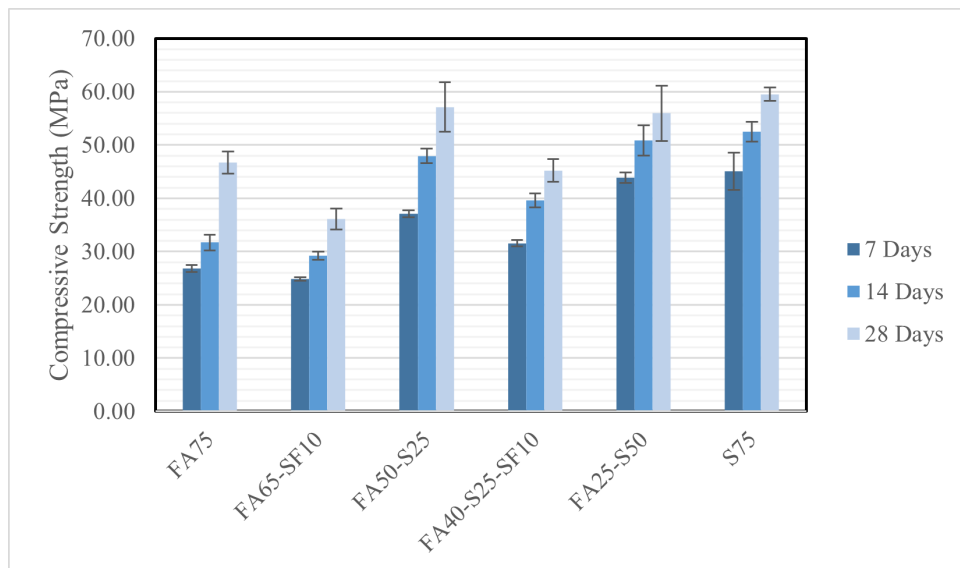


Figure 3. Compressive strength of 75% cement replacement with FA, S, and SF.

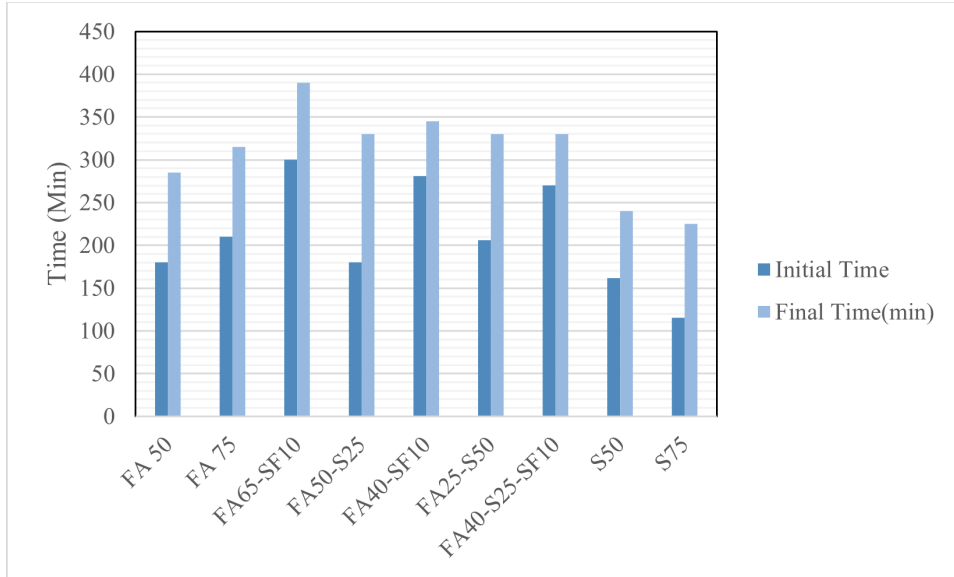


Figure 4. Setting time results of different ECC mixtures

3.4. Conclusion

This paper is a preliminary study in developing ECC mixtures that could be used for the 3D-printing application. ECC mortars were produced using locally available admixtures, including slag, fly ash, and silica fume, in region 6. The fiber content for all ECC mixtures was 1.5% (vol.). The cement was replaced with a combination of mineral admixtures in two substitution levels (i.e., 50% and 75%). The amount of water was adjusted somehow to result in a 19-20 cm flow table result and ensure the flowability/extrudability of the designed mixtures for the 3D-printing. The authors will do further research to complete this study in the next phase of their project. The preliminary study's collected results will provide the basis for our future research in the design of printable ECC mixtures. Overall conclusions drawn from this study are as follows:

The spherical shape of fly ash particles improved the workability of the fresh ECC mixtures. It led to a lower adjusted W/B ratio of fly ash-rich ECC (i.e., FA50 and FA75), while the slag-rich ECC mixtures (i.e., S50 and S75) required more water to reach a 19-20 cm flow table.

Incorporation of fly ash in ECC enhanced the fresh properties of the mixtures and the dispersion of the fibers in the fresh mixture while sliding of spherical particles in fly ash-rich mixtures (such as FA75) would lower the interlocking and load transition capability of the material and lowered their mechanical performance as it was observed for FA75 compared to FA50.

The highest compressive strength was obtained for 50% substitution of cement by slag or fly ash, which indicates the influential role of cement on the strength development of ECC mixtures.

The slag-rich ECC mixtures resulted in the shortest setting time and largest compressive strength than those of other designed mixtures. Slag contains a large content of calcium oxide, which would cause rapid setting with larger C- S-H precipitation at an early age, increasing the compressive strength of slag-rich mixtures.

The inclusion of silica fume lowered the compressive strength of ECC mixtures in combination with fly and slag and extended the setting time of fresh mixtures.

3.5. ACKNOWLEDGMENTS

The authors gratefully acknowledge the financial support from the Tran Set under Award # 20CUNM05. Any opinions, findings and conclusions or recommendations expressed in this material are those of the authors and do not reflect the views of the Tran Set view. The authors would like to thank for the invaluable assistance of Ms. Michele Anderson in laboratory work. All tests were performed in the Dana C. Wood Materials and Structures Lab at UNM.

3.6. REFERENCES

ASTM C305-20, Standard Practice for Mechanical Mixing of Hydraulic Cement Pastes and Mortars of Plastic Consistency, ASTM International, West Conshohocken, PA, 2020, www.astm.org

ASTM C109 / C109M-20, Standard Test Method for Compressive Strength of Hydraulic Cement Mortars (Using 2-in. or [50-mm] Cube Specimens), ASTM International, West Conshohocken, PA, 2020, www.astm.org

ASTM C1437-20, Standard Test Method for Flow of Hydraulic Cement Mortar, ASTM International, West Conshohocken, PA, 2020, www.astm.org

ASTM C125-15b, Standard Terminology Relating to Concrete and Concrete Aggregates, ASTM International, West Conshohocken, PA, 2015, www.astm.org

ASTM C191-08, Standard Test Methods for Time of Setting of Hydraulic Cement by Vicat Needle, ASTM International, West Conshohocken, PA, 2008, www.astm.org

- [1] S. Chaves Figueiredo *et al.*, “An approach to develop printable strain hardening cementitious composites,” *Mater. Des.*, vol. 169, 2019, doi: 10.1016/j.matdes.2019.107651.
- [2] D. G. Soltan and V. C. Li, “A self-reinforced cementitious composite for building-scale 3D printing,” *Cem. Concr. Compos.*, vol. 90, pp. 1–13, 2018, doi: 10.1016/j.cemconcomp.2018.03.017.
- [3] A. Perrot, Y. Mélinge, D. Rangeard, F. Micaelli, P. Estellé, and C. Lanos, “Use of ram extruder as a combined rheo-tribometer to study the behaviour of high yield stress fluids at low strain rate,” *Rheol. Acta*, vol. 51, no. 8, pp. 743–754, 2012, doi: 10.1007/s00397-012-0638-6.
- [4] R. J. M. Wolfs, F. P. Bos, and T. A. M. Salet, “Early age mechanical behaviour of 3D printed concrete: Numerical modelling and experimental testing,” *Cem. Concr. Res.*, vol. 106, no. January, pp. 103–116, 2018, doi: 10.1016/j.cemconres.2018.02.001.

- [5] Y. Weng *et al.*, “Printability and fire performance of a developed 3D printable fibre reinforced cementitious composites under elevated temperatures,” *Virtual Phys. Prototyp.*, vol. 14, no. 3, pp. 284–292, 2019, doi: 10.1080/17452759.2018.1555046.
- [6] A. Kazemian, X. Yuan, E. Cochran, and B. Khoshnevis, “Cementitious materials for construction-scale 3D printing: Laboratory testing of fresh printing mixture,” *Constr. Build. Mater.*, vol. 145, pp. 639–647, 2017, doi: 10.1016/j.conbuildmat.2017.04.015.
- [7] A. Albar, M. Chougan, M. J. Al- Kheetan, M. R. Swash, and S. H. Ghaffar, “Effective extrusion-based 3D printing system design for cementitious-based materials,” *Results Eng.*, vol. 6, 2020, doi: 10.1016/j.rineng.2020.100135.
- [8] N. Roussel, J. Spangenberg, J. Wallevik, and R. Wolfs, “Numerical simulations of concrete processing: From standard formative casting to additive manufacturing,” *Cem. Concr. Res.*, vol. 135, no. April, p. 106075, 2020, doi: 10.1016/j.cemconres.2020.106075.
- [9] V. Li, *Engineered Cementitious Composites (ECC): Bendable Concrete for Sustainable and Resilient Infrastructure*. 2019.
- [10] V. C. Li, “Engineered cementitious composite (ecc): Material, structural, and durability performance,” *Concr. Constr. Eng. Handbook, Second Ed.*, pp. 1001–1048, 2008.
- [11] M. B. Weimann and V. C. Li, “Hygral Behavior of Engineered Cementitious Composites (ECC),” *Int. J. Restor. Build. Monum.*, vol. 9, no. 5, pp. 513–534, 2003.
- [12] L. C. Li VC, “Theory of steady state and multiple cracking of random discontinuous fiber reinforced brittle matrix composites,” *Eng Mech-ASCE*, vol. 118, no. 11, pp. 2246–64, 1992.

- [13] E. H. Yang, S. Wang, Y. Yang, and V. C. Li, “Fiber-bridging constitutive law of engineered cementitious composites,” *J. Adv. Concr. Technol.*, vol. 6, no. 1, pp. 181–193, 2008, doi: 10.3151/jact.6.181.
- [14] R. Ranade, “Advanced Cementitious Composite Development for Resilient and Sustainable Infrastructure. PhD thesis,” p. 419, 2014.
- [15] V. C. Li, *Engineered Cementitious Composites (ECC)*. Berlin, Heidelberg: Springer Berlin Heidelberg, 2019.
- [16] D. Marchon, S. Kawashima, H. Bessaies-Bey, S. Mantellato, and S. Ng, “Hydration and rheology control of concrete for digital fabrication: Potential admixtures and cement chemistry,” *Cem. Concr. Res.*, vol. 112, no. December 2017, pp. 96–110, 2018, doi: 10.1016/j.cemconres.2018.05.014.
- [17] V. C. Li *et al.*, “On the emergence of 3D printable Engineered, Strain Hardening Cementitious Composites (ECC/SHCC),” *Cem. Concr. Res.*, vol. 132, no. April, p. 106038, 2020, doi: 10.1016/j.cemconres.2020.106038.
- [18] V. C. Li *et al.*, “On the emergence of 3D printable Engineered, Strain Hardening Cementitious Composites (ECC/SHCC),” *Cem. Concr. Res.*, vol. 132, no. January, p. 106038, 2020, doi: 10.1016/j.cemconres.2020.106038.
- [19] Z. Li *et al.*, “Fresh and hardened properties of extrusion-based 3D-printed cementitious materials: A review,” *Sustain.*, vol. 12, no. 14, pp. 1–33, 2020, doi: 10.3390/su12145628.
- [20] N. Roussel, “Rheological requirements for printable concretes,” *Cem. Concr. Res.*, vol. 112, no. March, pp. 76–85, 2018, doi: 10.1016/j.cemconres.2018.04.005.

- [21] S. Lim, R. A. Buswell, T. T. Le, S. A. Austin, A. G. F. Gibb, and T. Thorpe, “Developments in construction-scale additive manufacturing processes,” *Autom. Constr.*, vol. 21, no. 1, pp. 262–268, 2012, doi: 10.1016/j.autcon.2011.06.010.
- [22] T. T. Le, S. A. Austin, S. Lim, R. A. Buswell, A. G. F. Gibb, and T. Thorpe, “Mix design and fresh properties for high-performance printing concrete,” *Mater. Struct. Constr.*, vol. 45, no. 8, pp. 1221–1232, 2012, doi: 10.1617/s11527-012-9828-z.
- [23] Z. Malaeb, H. Hachem, A. Tourbah, T. Maalouf, N. El Zarwi, and F. Hamzeh, “3D Concrete Printing: Machine and Mix Design,” *Int. J. Civ. Eng. Technol.*, vol. 6, no. April, pp. 14–22, 2015, [Online]. Available: http://www.researchgate.net/profile/Farook_Hamzeh/publication/280488795_3D_Concrete_Printing_Machine_and_Mix_Design/links/55b608c308aec0e5f436d4a1.pdf.
- [24] G. W. Ma, L. Wang, and Y. Ju, “State-of-the-art of 3D printing technology of cementitious material—An emerging technique for construction,” *Sci. China Technol. Sci.*, vol. 61, no. 4, pp. 475–495, 2018, doi: 10.1007/s11431-016-9077-7.
- [25] Y. Zhang, Y. Zhang, G. Liu, Y. Yang, M. Wu, and B. Pang, “Fresh properties of a novel 3D printing concrete ink,” *Constr. Build. Mater.*, vol. 174, pp. 263–271, 2018, doi: 10.1016/j.conbuildmat.2018.04.115.
- [26] Y. Ding, J. tao Yu, K. Q. Yu, and S. lang Xu, “Basic mechanical properties of ultra-high ductility cementitious composites: From 40 MPa to 120 MPa,” *Compos. Struct.*, vol. 185, pp. 634–645, 2018, doi: 10.1016/j.compstruct.2017.11.034.
- [27] I. Curosu, V. Mechtcherine, and O. Millon, “Effect of fiber properties and matrix composition on the tensile behavior of strain-hardening cement-based composites (SHCCs)

- subject to impact loading,” *Cem. Concr. Res.*, vol. 82, pp. 23–35, 2016, doi: 10.1016/j.cemconres.2015.12.008.
- [28] D. Y. Lei and L. P. Guo, “Physical and mechanical properties of ultra-high strength and high ductility cementitious composites,” in *RILEM Bookseries*, 2018, vol. 15, pp. 211–220, doi: 10.1007/978-94-024-1194-2_25.
- [29] H. Ogura, V. N. Nerella, and V. Mechtcherine, “Developing and testing of Strain-Hardening Cement-Based Composites (SHCC) in the context of 3D-printing,” *Materials (Basel)*., vol. 11, no. 8, pp. 1–18, 2018, doi: 10.3390/ma11081375.
- [30] Y. Zhu, Z. Zhang, Y. Yang, and Y. Yao, “Measurement and correlation of ductility and compressive strength for engineered cementitious composites (ECC) produced by binary and ternary systems of binder materials: Fly ash, slag, silica fume and cement,” *Constr. Build. Mater.*, vol. 68, pp. 192–198, 2014, doi: 10.1016/j.conbuildmat.2014.06.080.
- [31] J. J. Chen, W. W. S. Fung, and A. K. H. Kwan, “Effects of CSF on strength, rheology and cohesiveness of cement paste,” *Constr. Build. Mater.*, vol. 35, pp. 979–987, 2012, doi: 10.1016/j.conbuildmat.2012.04.037.
- [32] Y. Bao *et al.*, “Three-dimensional printing multifunctional engineered cementitious composites (ECC) for structural elements,” *RILEM Bookseries*, vol. 19, pp. 115–128, 2019, doi: 10.1007/978-3-319-99519-9_11.
- [33] B. Zhu, J. Pan, B. Nematollahi, Z. Zhou, Y. Zhang, and J. Sanjayan, “Development of 3D printable engineered cementitious composites with ultra-high tensile ductility for digital construction,” *Mater. Des.*, vol. 181, no. July, p. 108088, 2019, doi: 10.1016/j.matdes.2019.108088.

- [34] M. Heikal and N. S. Ibrahim, “Hydration, microstructure and phase composition of composite cements containing nano-clay,” *Constr. Build. Mater.*, vol. 112, pp. 19–27, 2016, doi: 10.1016/j.conbuildmat.2016.02.177.
- [35] N. A. Tregger, M. E. Pakula, and S. P. Shah, “Influence of clays on the rheology of cement pastes,” *Cem. Concr. Res.*, vol. 40, no. 3, pp. 384–391, 2010, doi: 10.1016/j.cemconres.2009.11.001.
- [36] E. H. Yang, Y. Yang, and V. C. Li, “Use of high volumes of fly ash to improve ECC mechanical properties and material greenness,” *ACI Mater. J.*, vol. 104, no. 6, pp. 620–628, 2007, doi: 10.14359/18966.
- [37] H. Noorvand, G. Arce, M. Hassan, T. Rupnow, and L. N. Mohammad, “Investigation of the Mechanical Properties of Engineered Cementitious Composites with Low Fiber Content and with Crumb Rubber and High Fly Ash Content,” *Transp. Res. Rec.*, vol. 2673, no. 5, pp. 418–428, 2019, doi: 10.1177/0361198119837510.
- [38] B. Panda and M. J. Tan, “Experimental study on mix proportion and fresh properties of fly ash based geopolymer for 3D concrete printing,” *Ceram. Int.*, vol. 44, no. 9, pp. 10258–10265, 2018, doi: 10.1016/j.ceramint.2018.03.031.
- [39] B. Panda, S. Ruan, C. Unluer, and M. J. Tan, “Improving the 3D printability of high volume fly ash mixtures via the use of nano attapulgite clay,” *Compos. Part B Eng.*, vol. 165, no. November 2018, pp. 75–83, 2019, doi: 10.1016/j.compositesb.2018.11.109.
- [40] D. N. Richardson, “Strength and Durability Characteristics of a 70% Ground Granulated Blast Furnace Slag (GGBFS) Concrete Mix,” vol. 2006, p. 94, 2006, [Online]. Available: <http://library.modot.mo.gov/RDT/reports/Ri99035/or06008.pdf>.

- [41] H. S. Lee, X. Y. Wang, L. N. Zhang, and K. T. Koh, “Analysis of the optimum usage of slag for the compressive strength of concrete,” *Materials (Basel)*., vol. 8, no. 3, pp. 1213–1229, 2015, doi: 10.3390/ma8031213.
- [42] J. K. Kim, J. S. Kim, G. J. Ha, and Y. Y. Kim, “Tensile and fiber dispersion performance of ECC (engineered cementitious composites) produced with ground granulated blast furnace slag,” *Cem. Concr. Res.*, vol. 37, no. 7, pp. 1096–1105, 2007, doi: 10.1016/j.cemconres.2007.04.006.
- [43] A. K. H. Kwan and Y. Li, “Effects of fly ash microsphere on rheology, adhesiveness and strength of mortar,” *Constr. Build. Mater.*, vol. 42, pp. 137–145, 2013, doi: 10.1016/j.conbuildmat.2013.01.015.
- [44] N. Roussel, G. Ovarlez, S. Garrault, and C. Brumaud, “The origins of thixotropy of fresh cement pastes,” *Cem. Concr. Res.*, vol. 42, no. 1, pp. 148–157, 2012, doi: 10.1016/j.cemconres.2011.09.004.
- [45] P. Norrarat, W. Tangchirapat, S. Songpiriyakij, and C. Jaturapitakkul, “Evaluation of Strengths from Cement Hydration and Slag Reaction of Mortars Containing High Volume of Ground River Sand and GGBF Slag,” *Adv. Civ. Eng.*, vol. 2019, 2019, doi: 10.1155/2019/4892015.

Chapter 4

4. Evaluation of Mechanical Properties of 3D-Printable Engineered Cementitious Composite

Abstract

Engineered cementitious composite (ECC) with high ductility is emerging as a promising material for 3D concrete printing (3DCP) applications. However, one of the challenges in the industry is achieving a high ductile ECC mix design. This paper investigated the mechanical performance of four novel mix designs casted by two methods, i.e., mold-cast and extrusion-based 3D printing using Polyvinyl alcohol (PVA) and Ultra-High Molecular Weight Polyethylene (PE) fibers in two fiber ratios of 1.5% and 2% of total volume. In addition, the compressive, direct tensile, and three-point bending tests were conducted on the ECC specimens. The influence of different parameters, including the effect of different admixtures, fiber volumes, and 3D printing parameters, were explicitly investigated. The results indicated that ECC samples containing PE fibers could achieve ultra-high ductility with a strain capacity of over 10% with an optimized mixing procedure and viscosity modifier addition. This study's results simultaneously expanded the boundary of developing ECC with high compressive strength and ductility.

Keywords: Engineered cementitious composites (ECC); Ultra-high ductile; Additive manufacturing (AM); 3D concrete printing (3DCP); Tensile strength; Flexural Strength; Mixing procedure; Sustainable development

4.1. Introduction

Digital manufacturing (DM) is growing in major industrial countries as the principle of future construction. DM, also called additive manufacturing (AM), layer manufacturing, or 3D printing, can surpass conventional construction circumscribes [1]. 3D printing technologies can reduce the carbon footprint by employing recycling methods, innovative organic materials, and proximity of production to consumers by transportation cost reduction.[2] A wide range of materials has been studied congruous with 3D printing in the different fields of the industry (i.e., aerospace, automotive, and medical) , including carbon fiber, metal, acrylonitrile butadiene styrene (ABS), alumide, nitinol [72,73]. However, when it comes to construction, aggregate-based materials, namely concrete, are the most popular materials for additive construction.[5] Pegna, in his exploratory work, employed a material deposition technique with different layers of Ordinary portland cement (POC) and sand to achieve a solid freeform fabrication in large structures.[6]. Despite the vast potential for using 3D printing in construction, some challenges exist in incorporating cementitious materials in 3D printing applications, limiting the broad application of this novel technology. These challenges include durability, reinforcement, forming cold joints between printed layers, anisotropic mechanical performance, and achieving proper fresh properties of 3D printable mixtures. Some of these issues have been studied and addressed over the past years [48,4,75]. Our previous studies illustrated that incorporating fibers and appropriate supplementary cementitious materials is a viable solution to overcome some of the current obstacles (i.e., fresh properties, and mechanical properties) in 3DCP applications [10][11][12].

Fiber reinforcement of concrete suitable for 3D printing has been recognized as a potentially suitable approach to overcome the brittle behavior of hardened concrete [25,35]. Past studies demonstrated that the capacity of ultra-high ductility cementitious composites (UHDFCC) with 2%

volume fraction of PE fibers can match the capacity of conventional reinforced concrete beams with a steel reinforcement ratio of 0.5–1.5% [15]. Therefore, numerous studies have been conducted to assess the compressive strength, tensile strength, and ductility of fiber-reinforced 3D printed concrete [16],[14],[17]. The invention of Engineered cementitious composite (ECC), known for its strain hardening behavior and microcracking, is a promising approach to overcoming mechanical properties' challenges in 3D concrete printing. Generally, two categories of Fiber Reinforced Concrete (FRC) and High-Performance Fiber Reinforced Cementitious Composites (HPFRCC) can be classified depending on the tensile ductility achieved along strain capacity. While FRC has a tension-softening behavior, HPFRCC is accompanied by a strain-hardening behavior. In addition, multiple microcracks accompany the deformation during strain-hardening of HPFRCC class material, resulting in significantly different load capacity and structural durability compared to FRC [18][19].

Fine aggregates have been accepted for ECC over coarse aggregate to achieve a better strain capacity and multiple cracking with less than 60 μm [20][21]. In addition, eliminating coarse aggregate from the ECC mix leads to a higher cement content than conventional concrete developed for structural members. However, the high cement content in ECC has numerous negative impacts (i.e., higher carbon dioxide, high hydration heat, higher cost, and negative impacts on the environment). Incorporating supplementary cementitious materials (i.e., Fly ash (FA) and Blast furnace slag (S)) provides the possibility of partial cement replacement and lowering the cement content used in ECCs. Numerous successful ECC mix designs have been developed with supplementary cementitious materials (i.e., FA, S, silica fume (SF), nano-clay (NC), metakaolin (MK)) commonly used as an alternative for partial cement replacement [22][23][24]. Some researchers have developed ECCs with a high volume of fly ash and slag

replacement (up to 85% replacement by weight) as an attempt to mitigate the environmental effect of concrete[25][26]. The replacement of portland cement with Slag to achieve the desired strength development ranges between 40%-60% [27][28].

The remarkable tensile ductility of ECC (i.e., several hundred times that of conventional concrete) with compressive strength similar to concrete or even high-strength concrete makes ECC an exceptional alternative for construction [19]. To improve the ductility of this material, a moderately low fiber volume fraction (e.g., less than 2%) of polyvinyl alcohol fibers (PVA) or polyethylene fibers (PE) are often used. Huang et al. [29] developed a high-strength, and high-ductility (HSHD) ECC using 2% by volume fraction 18mm PE fibers with an ultimate tensile strength of 12 Mpa and an ultimate tensile strain of 11% for cast specimens. Moreover, Li et al. developed a high-strength and high-ductility engineered cementitious composite (HSHD-ECC) using coarse river sand (RS) for the first time using 2% by volume fraction 18mm PE fibers. The compressive strength of ECC exceeded 115 MPa, and the tensile strength and strain of 12 MPa and 9%, respectively [29].

Incorporating fibers in ECC to possess self-reinforcement properties makes it a great candidate for the 3D printing of infrastructure systems Soltan and Li investigated the printability of several compositional ingredients and processing parameters of ECC and demonstrated that the ECC could be adapted for 3D printing applications [14]. Moreover, Zhu et al. [30] aimed for a high tensile strain capacity (i.e., over 8% strain capacity) 3D printed ECC with 12mm PE fibers (2% of total volume), and the product was a mix with 11.43% strain capacity and 5.35 Mpa tensile strength. Additionally, Soltan and Li [14] demonstrate that 3D printed ECC can outperform cast one using 12 mm PVA fibers and developed a 3D printed ECC with tensile strength and tensile strain capacity of 5 MPa and 4%, respectively. Recently Zhou et al. have improved the tensile strength

and capacity of ECC by adjusting the nozzle standoff distance, achieving a 3D printed ECC with 7Mpa tensile strength and 4% strain capacity using 12mm PE fibers[31]. It is worth noting that the length of the fibers is cited for each study along the fiber types as it can impact the typical failure mode (i.e., pullout and rupture) of ECC. Huang et al. demonstrated that the failure model alters from pullout to rupture mode with increasing fiber length [32].

This paper is a continuation of previous research [10][11][12] to investigate the feasibility and adaptation of ECC for 3D printing applications. Previously, the mix design and printability of ECC mixes were studied comprehensively. The effect of using different SCMs, and incorporating viscosity modifying admixture (VMA) on fresh characteristics of designed ECC mixes, their printability aspects (i.e., buildability and extrudability), and printing system (i.e., printing and extrusion speed) were studied. Accordingly, an appropriate approach was implemented by adding Methylcellulose (MC) as a VMA to adapt fresh properties of designed ECC mixes for printing. As a result, superior rheological properties and better fiber dispersion were achieved by MC incorporation, resulting in a promising quality of the 3D printed objects. However, few studies have been performed on improving the strain capacity of ECC suitable for 3D printing, considering the quantity and the type of fibers. Therefore, this study investigates the mechanical performance of selected ECC mixes from our previous studies to evaluate their mechanical properties (i.e., flexural test, tensile test, and compressive test), and compare it with the cast-in-place ECC mixes. This study explores the effect of ECC mix design, different fiber types (PVA vs. PE) and volumetric fiber contents (1.5% and 2%) on the mechanical properties of ECC mixes.

4.2. Methods and materials

4.2.1. Materials and mix designs

Four ECC mixes in this study were adapted from our previous research [10][11][12]. They were a combination of 50% type I/II ordinary portland Cement (C) and 50% mix of other mineral admixtures, including Silica Fume (SF), Class-F Fly Ash (FA), Ground Granulated Blast Furnace Slag (S), and Metakaolin (MK). Table 4 displays the chemical compositions of given mineral admixtures.

ECC mixes were internally reinforced using two types of fibers, non-oil coated RECS15 PVA and ultra-high-molecular-weight PE, and at two volumetric contents (i.e., 1.5% and 2% by the volume of the mixture). The properties of fibers are illustrated in table 2. From the fiber properties, it is notable that they have a similar length, while PE fibers are 63% thinner than PVA fibers and the tensile and flexural strengths of PE fibers are 1.9 and 2.5 times, respectively, larger than the strengths of PVA ones.

These ECC mixes contained 25% (by weight) river sand (RS) with a fineness modulus of 2.3 and a maximum particle size of 3.36, which has been used as per ASTM C330. Additionally, the bulk dry specific gravity and absorption capacity of RS were 2.59 and 0.44%, respectively. Table 2 presents the sieve analysis (ASTM C136-14) results and properties of sand.

The ECC mixtures also include a polycarboxylate-based High Range Water Reducer (HRWR), ADVA 195, supplied by GCP-applied technologies, that complies with the ASTM C494. Additionally, according to our previous research findings, Methylcellulose (MC) was used in the mix designs as a VMA by 0.01 of the binder ratio.

Four ECC mortars were designed, as shown in Table 6. The mixes were named FA50 (representing 50% weight of C replaced with FA), S50 (representing 50% weight of C replaced with S), FA40-

SF10 (representing a binder FA50 but with 10% weight of FA replaced with SF), and FA40-MK10 (representing a binder identical to F but with 10% weight of FA replaced with MK).

Table 4. Chemical composition of mineral admixtures

Material	SiO ₂	Al ₂ O ₃	Fe ₂ O ₃	CaO	MgO	SO ₃	K ₂ O	TiO ₂	Na ₂ O	Specific Gravity
C	19.24	4.75	3.35	65.80	2.20	3.61	0.54	0.21	-	3.13
S	30.80	11.45	2.26	47.50	3.65	3.03	0.38	-	0.17	2.91
SF	97.80	-	-	-	-	0.30	-	-	0.01	2.20
FA	61.27	23.18	5.09	2.11	1.19	0.30	1.43	-	1.44	2.09
MK	53.00	43.80	0.43	0.02	0.03	0.03	0.19	1.70	0.23	2.5

Table 5. Properties of PVA and PE fibers

Material	Diameter (microns)	Length (mm)	Specific Gravity	Tensile Strength (MPa)	Flexural Strength (GPa)	Color
PVA Fibers	38	8	1.30	1600	40	White
PE Fibers	15	8	0.97	3000	100	White

Table 6. Mix design of different ECC mixtures

#	Mix ID	Fiber Type	C/B	FA/B	S/B	SF/B	MK/B	W/B	Adjusted W/B	RS/B	MC (%) ¹	HR WR (%) ¹	Fibers (Vol%) ³
1	FA50	PVA	0.5	0.5	0	0	0	0.27	0.23	0.25	0.01	0.006	1.5
		PVA									0.01		2
		PE									0.01		2
2	S50	PVA	0.5	0	0.5	0	0	0.27	0.30	0.25	0.01	0.006	1.5
		PVA									0.01		2
		PE									0.01		2
3	FA40-SF10	PVA	0.5	0.4	0	0.1	0	0.27	0.27	0.25	0.01	0.006	1.5
		PVA									0.01		2
		PE									0.01		2
4	FA40-MK10	PVA	0.5	0.4	0	0	0.1	0.27	0.27	0.25	0.01	0.006	1.5
		PVA									0.01		2
		PE									0.01		2

Note: 1. %HRWR and MC dosage by weight of Binder

2. C: Cement; FA: Fly Ash; S: Slag; MK: Metakaolin; SF: Silica Fume; W: Water; RS: River Sand; B: Binder; HRWR: High Range Water Reducer, MC: Methyl Cellulose

3. all ratios are weight (wt) ratios but the volumetric fiber content.

4.2.2. Mixing procedure

The mixing procedure of ECCs plays an important role in their fresh/hardened properties since the large quantity of fiber makes achieving a consistent mix very hard. Undesirable mix consistency before adding fibers may cause poor fiber distribution and result in inferior hardened properties, especially ductility.[33]. Our previous study [] shows the crucial role of MC in the even distribution of fibers in ECC mixes, and a step-wise mixing procedure was adapted for this study to achieve the best consistency as listed here and schematically displayed in Figure 6:

Stage-I: All the dry powders (i.e., C, FA, S, SF, MC, and RS) were dry-mixed for 10 min constantly at low speed (140 ± 5 RPM) in a Hobart mixer.

Stage-II: The liquid form HRWR was added to dissolve in the water separately, and then the developed solution was added to the premixed dry powders slowly. The mixing continued for another 5 mins at the same speed (i.e., 140 ± 5 RPM).

Stage-III: Finally, the fibers (i.e., PVA and PE) were added to the blended mix, and the mixing continued for another 5 min at a low speed (i.e., 140 ± 5 RPM), followed by 5 minutes of mixing at a higher speed of 285 ± 10 RPM.

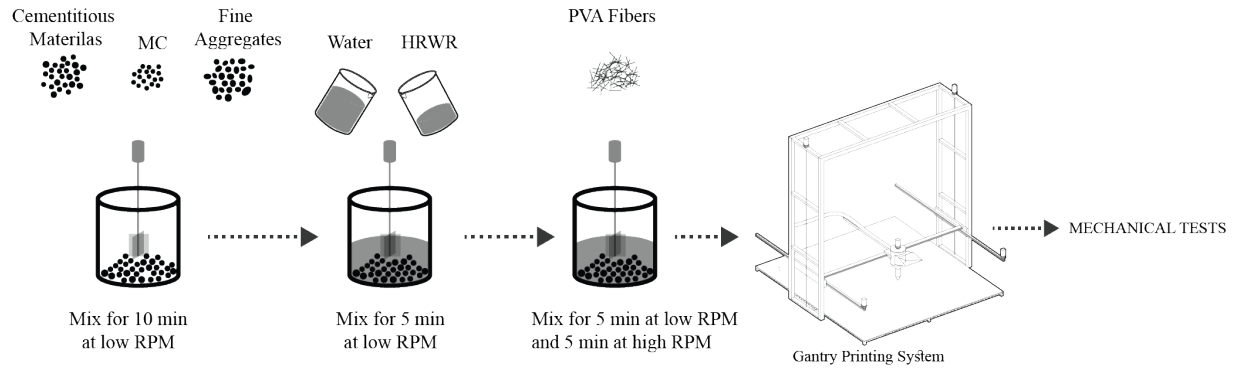


Figure 5. Mixing procedure of ECC Mixtures

4.2.3. 3D printing setup

A gantry 3D printer system was used to 3D print the specimens for mechanical testing. The gantry system in hand can move in the three principal axes in a straight line. The maximum reach of the system is $2 \times 2 \times 2$ m. In addition, the system is equipped with a hopper above the nozzle to adjust the extrusion speed and ensure the consistency of the filament while printing. The hopper is mounted to a one-stage pump-mixer by a 50 mm diameter circular hose that allows the mixing of fresh materials in a batch and pumping. The nozzle size is adjustable, but for the produced samples, a 20mm diameter circular shape nozzle has been used to increase the accuracy of printed objects. The extrusion speed of the hopper can reach up to 50RPM, and the maximum printing speed can reach up to 50 mm/s. The tool paths produced for the 3D printer are in G-code format, and simplify3d software has been used as slicing software to produce the desired geometries.

4.3. Test Methods

This study aimed to evaluate the mechanical properties and ductility of the extrudable and buildable ECC mixtures designed in the previous phase, and their fresh properties are adjusted for 3D printing. Furthermore, in this study, the assessment of ECC ductility as a function of different admixtures, fiber contents, and fiber types has been carried out. The compressive strength, direct tensile, and three-point bending tests were conducted on the ECC specimens. The influence of

different parameters, including ECC mix design (utilizing different admixtures), fiber volumes, types, and production method (Casting vs. 3D printing) was explicitly investigated. A short review of mechanical test methods is presented in the following sections.

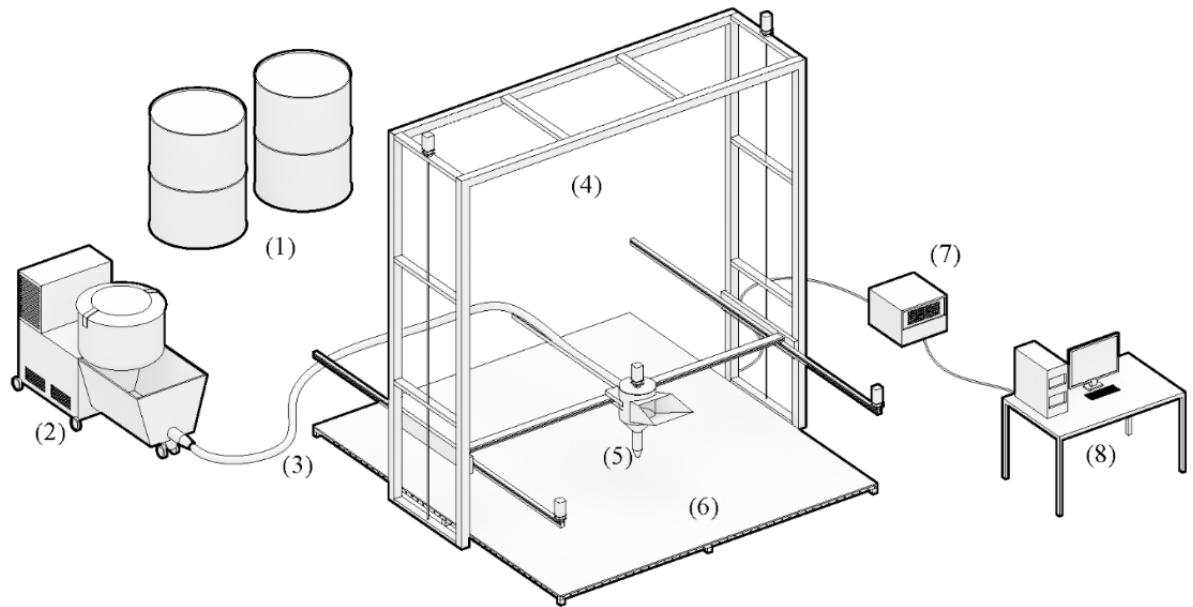


Figure 6. Raw materials (1), Mixer and Pump assembly (2), 3 inches diameter hose (3), 3D printer frame (4), Printing nozzle (5), 2x2 Printing bed (6), 3D printer processor (7), PC with software (8)

4.3.1. Compressive Strength of Cast Samples

The compressive strength of cast samples was evaluated to ensure the viability of using the designed ECC for structural applications. Three cubic samples of 50×50×50 mm were prepared according to ASTM C109-20. The casted cubes were cured in a moist room (100% RH, 23±0.5°C) 24 hours after preparation and kept there up to the age of 28-day to perform the compressive test. A Forney compression testing machine with a maximum capacity of 400 kips and a ramp rate of

100 psi/s, as shown in Figure 8. (3), was used to obtain the test results. to assess the effect of 3D printing on compressive strength

4.3.2. Compressive Strength of 3D Printed Samples

To study the mechanical properties of the 3D-printed component and pore formation between printed layers, designed ECC mixes containing PVA fibers were tested for compressive strength. From each mix, a 150×150×60 mm prism was printed using the gantry system with a 20 mm in diameter nozzle. The samples were transferred to a moist room (100% RH, 23±0.5°C) 24 hours after printing and kept there until testing at 28-day. Before testing, four small cubes of 50×50×50 mm were extracted from the preliminary 3D-printed object using a wet saw. All samples were tested perpendicular to the printing direction. The cubes were tested after 28 days at a loading rate of 100 psi/s according to ASTM C109-20. Figure 8 displays the printed specimen before and after cutting, and during the compression tests.



Figure 7. Primary 3D printed 150×150×60 mm sample with 20mm circular nozzle (1), four extracted 50×50×50mm cubic specimens from the primary sample (2), Compressive test setup with samples tested perpendicular to the loading direction (3)

4.3.3. Flexural strength of 3D printed samples

A three-point bending test was conducted according to the ASTM C 348-02 to evaluate the flexural strength of different mixes; Figure 9 illustrates the test setup and samples. A primary slab of 100×350×50mm was 3D printed using a 20 mm diameter nozzle. The 3D-printed slab was placed in a moist room (100% RH, 23±0.5°C) after 24 hours of printing, and they were kept there until the testing day. Before testing, four prisms of 40×40×160 mm were extracted from the primary 3D-printed prism. An Instron universal testing machine with an applied load of 0.5 mm/min was used to test the specimen, and the mounted LVDT to the setup measured the deflection of samples.

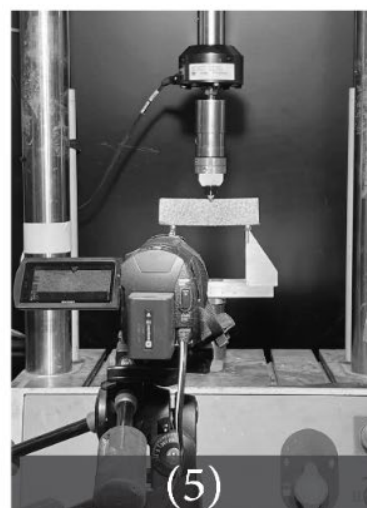
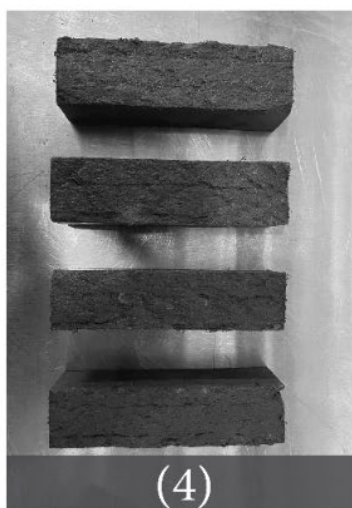
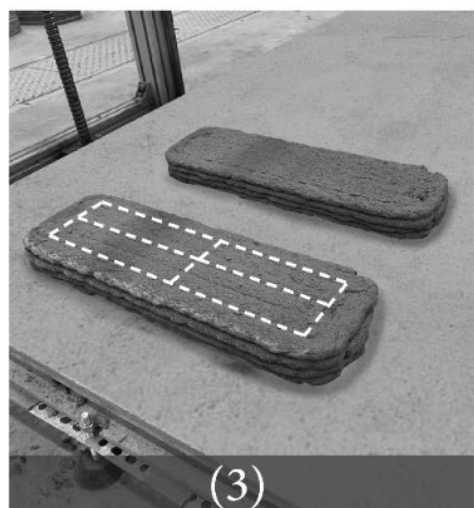
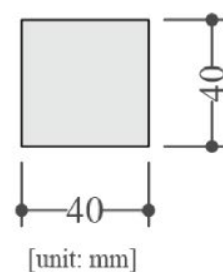
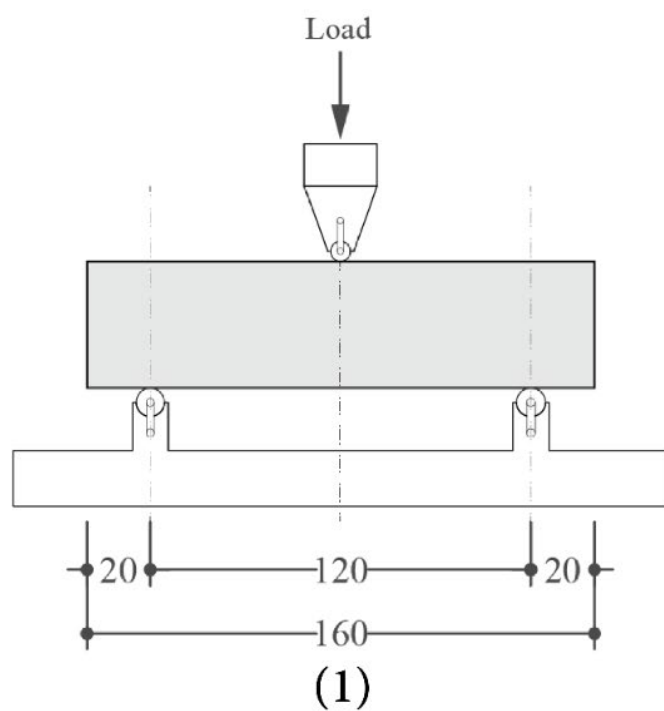


Figure 8. Three-point bending schematic test setup (1), the cross-section of the tested beam (2), primary 3D Printed slab of 100×350×50 mm with 20 mm circular nozzle (3), four extracted 140×40×40 mm beams from the primary slab (4), the third point bending test setup (5)

4.3.4. Uniaxial direct tensile test

This test measured the tensile strength of 3D printed dog bone samples as shown in Figure 10. The dog-bone samples' dimensions and thickness were according to the Japan Society of Civil Engineers (JSCE) recommendation [34]. Figure 6 illustrates the test setup and the dimension of the samples prepared for the direct tensile test. The fiber orientation of cast and 3D-printed ECC varies, affecting the test specimens' mechanical properties. Therefore, all samples were 3D printed using a 30 mm diameter nozzle to maintain the fiber orientation. Since 3D printing of the standard dog bone geometry is demanding, and even 3D printing a larger slab and cutting dog-bone shape samples from it to get a standard specimen would be challenging and needs special equipment, a different approach was adopted in this study. In this method, then the central part of the dog-bone specimen was printed, and the rest of the mold was filled with fresh ECC. The cross-section of the central part of the specimen under tensile load is 30×13 mm. For printed ECC, a filament with a 30 mm width and 13 mm thickness was printed in the mold, and the rest of the mold was filled and cast with ECC to shape the dog-bone samples. The printed specimens were prepared and kept in a moisture room (100% RH, $23 \pm 0.5^\circ\text{C}$) for 28 days. The uniaxial direct tensile test was performed using an MTS Bionix servo-hydraulic universal testing machine with an applied load of 0.5 mm/min, according to JSCE. Two external linear variable displacement transducers (LVDTs) were fixed to a rigid plastic frame to measure elongation. The average value of two LVDTs was considered to calculate the tensile strain. Three specimens were prepared, and the mechanical property was averaged for each ECC mix.

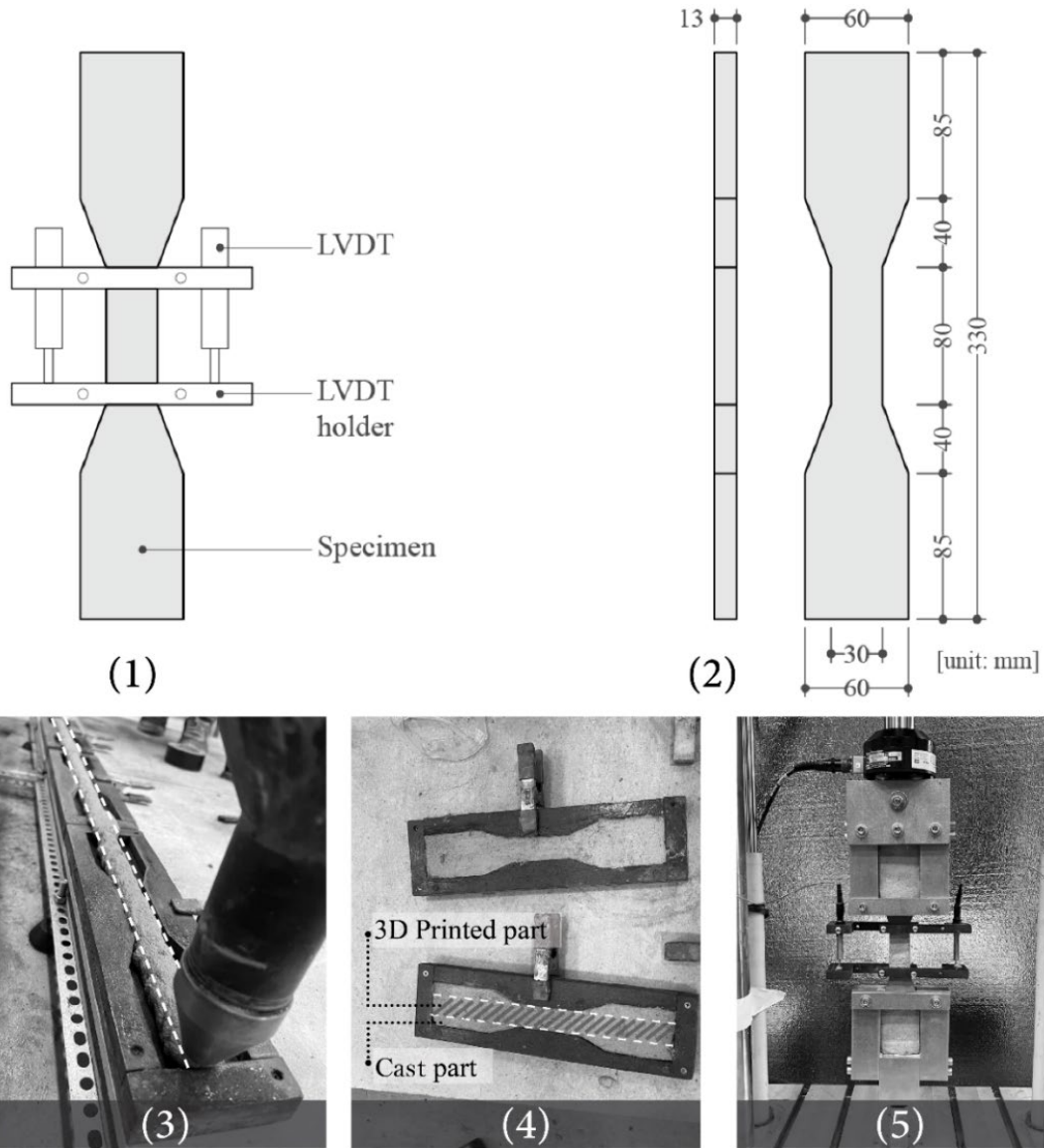


Figure 9. Uniaxial direct tensile test schematic test setup (1), dimension of dog-bone 3D printed samples (2), 3D printing the specimen inside the molds for under tension area (3), specimen showing 3D printed and cast part (4), test setup (5)

4.4. Results and Discussion

The results of different mechanical test methods are presented in this section.

4.4.1. Compressive test results

The compressive strength development of cubic samples after 28 days of age are illustrated in Figure 11. Each data point averages the results of three and four specimens for the cast and 3D-printed ones, respectively. Figure 11 compares the results of cast versus (vs) 3D printed specimens, different ECC mixes, different PVA fiber content, and types of fibers (2% of PVA vs. PE). The data interpretation of the compressive strength is listed below:

The results of ECC mixes containing 1.5% PVA fibers are presented for both cast, and 3D printed specimens to evaluate the effect of 3D printing on the mechanical properties of the developed specimens (Figure 11-(1)). Overall, the compressive strength of 3D printed cubes was lower compared to the cast ones. According to Figure 11-(1), using 1.5% PVA fibers, the compressive strength of the cast specimens was in the 53.5-59.0 MPa range, while for the 3D-printed cubes, this strength range was dropped to 35.15-50.0 MPa. FA50-1.5PVA exhibited the max compressive strength reduction of 36% for cast vs. 3D-printed specimens. The compressive strength of cast FA40-MK10-1.5%PVA, FA40-SF10-1.5%PVA, and S50-1.5%PVA decreased for the 3D-printed samples by 28%, 34%, and 15%, respectively. This compressive strength reduction could be attributed to forming voids between extruded filaments (i.e., inter-filament voids) [35]. These voids in the printed structures act as defects and adversely influence the hardened properties of the 3D-printed specimens. Previous research [36][16] showed a similar trend and a reduction in the compressive strength of 3D-printed materials because of the introduced air voids between two adjacent layers by the extrusion-based 3D printing process, which might weaken the load-bearing capacity of ECC to some extent. Generally, printed layered structures are presumed to be anisotropic due to the forming of voids between the filaments and between layers. As a result, a

weak bond between the layers or void presence along the printing direction due to the poorly executed printing process can weaken the compressive strength of printed objects depending on the applied load direction.

Figure 11 (1) and (2) shows the effect of using different admixtures (i.e., F, MK, SF, and S) in the mix design of ECC on the compressive strength development. Overall, the lower compressive strength was associated with the FA-rich mixes (i.e., FA50, FA40-MK10, and FA40-SF10), while S50 showed the maximum compressive strength in all 1.5%PVA and 2% of PVA and PE fibers cases. The larger strength of S50 could be caused by slag particles containing significant calcium oxide content, which would cause rapid setting with larger C-S-H precipitation at an early age, improving the compressive strength of slag-rich mixtures. Replacing FA with MK or SF led to larger compressive strength and, at 2%PVA, improved the compressive strength of FA50 by 10% and 14% for FA40-MK10 and FA40-SF10, respectively. These results indicate that MK and SF incorporation would improve the compressive strength of ECC mixes after 28 days regardless of having a higher W/B ratio compared to FA50. In addition, MK and SF with a filling effect can densify the mix and overall compactness, resulting in higher compressive strength. MK is also a pozzolanic material. The reaction between Al_2O_3 and SiO_2 from MK and CH generated during hydration could enhance the amount of C-S-H gel in the matrix, increasing compressive strength[22][37]. Figure 11 displays the results of four ECC mixes at 1.5 and 2 % fiber content. From Figure 11-(1), the maximum strength of 3D-printed cubes was observed for S-50 (i.e., 50.0 MPa), while the minimum strength was reported for F-50 (i.e., 35.15 MPa).

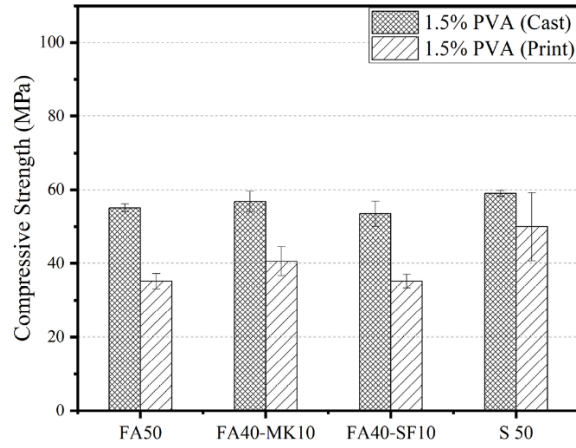
Increasing the PVA fiber quantity from 1.5% to 2% improves the compressive strength of ECC in all cases except FA50, which was reduced 10%. This compressive strength reduction in FA50 could be attributed to increased porosity with increasing fiber content. As mentioned before,

introducing MK and SF in ECC can densify the matrix, reduce the porosity and improve fiber-matrix bonding strength. As a result, unlike FA50, higher fiber contents improved the compressive strength of MK and SF-rich mixtures. For S50, compressive strength of 3D-printed cubes enhanced 60 % by increasing PVA fiber from 1.5% to 2% and showed the maximum strength improvement by adding more fibers. Previous studies [38][39][40] were in disagreement with observed trend and showed a higher quantity of fibers tends to decrease the compressive strength. As reported by Z. Pan et al.[38], the effect of fiber contents on the compressive strength of a specimen can be originated from two opposite aspects. The positive aspect is that the compressive strength can be improved by developed restrains of lateral expansion under loading due to fiber bridging leading to microcrack sliding and extending. The negative aspect is that increasing the fiber content increases ECC's porosity and density, leading to strength loss. However, the addition of MC in this study improved ECC's consistency with 2% fibers in the fresh state and led to the formation of denser materials in the later ages for all designed ECC mixes except FA50.

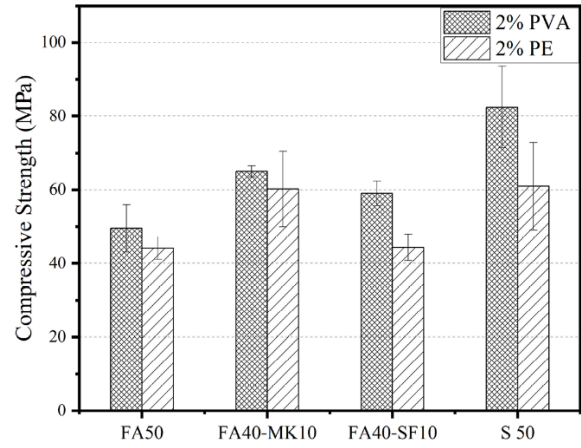
Figure 11-(2) demonstrates the compressive strength of ECC mixes containing 2% PVA vs. 2% PE fibers to assess the effect of fiber type on the compressive strength development of ECC mixtures after 28 days. Replacing PVA with PE in mixes containing 2% fibers reduces compressive strength in all cases. The compressive strength of ECC mixes with 2%PVA fibers was in the range of 49.6-82.5 MPa, while this strength range decreased to 42-60 MPa for the incorporation of 2%PE fibers. The maximum strength reduction by utilizing different types of fibers was for S50, and its strength was reduced by 26% after replacing PVA fibers with PE ones. This lower compressive strength for PE fiber could be explained by the physical properties of PE fibers shown in Table 5. The diameter of PE fibers is 1/3 of PVA fibers leading to a higher number of fiber quantities of the same weight. Therefore, the reduction in the compressive strength of PE

mixes compared to PVA can be attributed to the higher number of PE fibers in ECC mixes which makes the PE mixes susceptible to higher porosity and lower density.

The results from the compressive strength test prove that a higher compressive strength with a higher fiber content is achievable by adopting appropriate approaches to improve fiber distribution. The fact that the compressive strength improved with increasing fiber contents demonstrates the performance of the adopted approach. Introducing a viscosity modifying agent (MC) and adjusting the mixing procedure was the adopted approach to achieve the desired fiber distribution leading to better mechanical performance. The higher standard deviation of specimens containing 2% fibers can be attributed to the inhomogeneous distribution of fibers, which tends to appear more with higher fiber contents. Including slag in fiber-reinforced concrete can enhance fiber dispersion, thereby improving the mechanical performance of ECC. This is because the slag particles contribute to the fibers' mortar matrix flow and dispersion.[41] In addition, the fact that S50-2%PVA had the highest compressive strength with 82.47 MPa proves that slag particles can improve the fiber distribution and ECC's compressive strength.



(1)



(2)

Figure 10. Compressive strength of specimen containing 1.5%PVA for cast and printed specimens at 28-day age (1), compressive strength of cast specimens containing 2%PVA and 2%PE for cast samples at 28 days of age (2)

4.4.2. Direct tensile test

Figure 12 presents the stress-strain curve from direct tensile tests of 3D-printed dogbone specimens at 28-day age and examines the effects of the ECC mix design, fiber content (1.5% vs. 2% PVA fibers), and fiber types (2% PVA vs. 2% PE fibers). For each mix, there were three repeats, and as shown, the results of the three tensile tests were in good agreement for all ECC mixes. Overall, the tensile stress-strain curve of all ECC mixes exhibits two regions, including the linear elastic region at the beginning of the curve, followed by the plastic portion of the curve, which is a strain-hardening region. Notably, all the specimens exhibited pseudo-strain hardening behavior and multiple cracking. Additionally, the numerical results of tensile properties of all ECC specimens after 28 days under the uniaxial direct tensile test are illustrated in Table 7. Moreover, from stress-strain curves, the yield stress and strain energy densities were computed as an approximate area under the stress-strain curve before yielding and after rupture and represented as the modulus of resilience, and toughness, respectively, in Table 8. Toughness is the material properties that

indicate the material's ability to resist plastic deformation up to rupture, and it is a good balance of ultimate strength and strain capacity (i.e., ductility).

The stress-strain results of different ECC mixes in Figure 12 indicate the higher ductility of S50 compared to other mixes. For 2%PVA and 2%PE fiber, the strain capacity of S50 is 1.34 and 1.4times larger than F50, respectively. In comparison, the ultimate tensile strength of FA50 specimens was 4.5% larger than that of S50. As such, the modulus of the toughness of S50 is 15% larger than FA50%. Slag can improve ECC mixtures' fiber distribution resulting in better ductility. Therefore, the superior strain capacity of S50-2%PE could be related to the good distribution of PE fibers inside the matrix resulting in a higher strain capacity. Substituting 10% of MK with FA in FA50 resulted in almost similar ultimate tensile strength, as reported in Table 7, while replacing FA with SF led to lower tensile strength. Regarding toughness for 2%PE fiber, the FA50 exhibited 15% smaller and 67% larger toughness compared to the toughness of FA40-MK10 and FA40-SF10, respectively. These findings indicate the ability of MK and S in absorbing energy. The first cracking strength is defined as the load at which the stress-strain curve deviates from linearity and the first cracking initiates. The first cracking strength, independent of age, initiates from the defect sites in ECC. The first cracking strength in 2% PE, S50, and FA40-MK10 is 20% and 80% lower, respectively, compared to corresponding mixes with 2% PVA fibers.

Increasing the PVA fiber contents from 1.5% to 2% enhances the strain capacity of all ECC mixes. FA50 exhibited minor change (i.e., 1.14% increase) in strain capacity while FA40-MK10 showed maximum change (i.e., 317% increase). Nevertheless, incorporation more PVA fibers led to improvement of ultimate tensile strength in all ECC but FA50. Furthermore, change of PVA content from 1.5% to 2% improved the toughness of ECC mixes but FA50 as shown in Table7.

FA50 containing 2% PE fibers exhibits 25% higher peak stress than the corresponding 2% PVA mix. The first cracking strength was increased slightly for FA50 and S50 with increasing the fiber dosage, which is in good agreement with other studies [39][42]. However, in the case of S50, the first cracking strength decreases as the fiber dosage increases. The specimens containing 2%PE have more fluctuation under tension, and the development of fiber bridging and strain hardening is more evident than in 1.5%PVA and 2%PVA mixes. The typical length of PVA fibers utilized for ECC is 12mm, whereas the PVA fibers used in this study are 8mm. Comparing the stress-strain curve of other studies related to PVA fiber-reinforced ECC revealed that 8mm PVA fibers were unsuitable for achieving the desired strain capacity and optimum fiber bridging. The toughness of 2% PE mixes is larger than 2% PVA in all cases. Replacing the PVA fiber types with PE improved the toughness of all mixes around six times except FA40-SF10. The lower performance of FA40-SF10 in toughness can be attributed to the low first cracking strength of SF-rich mixtures.

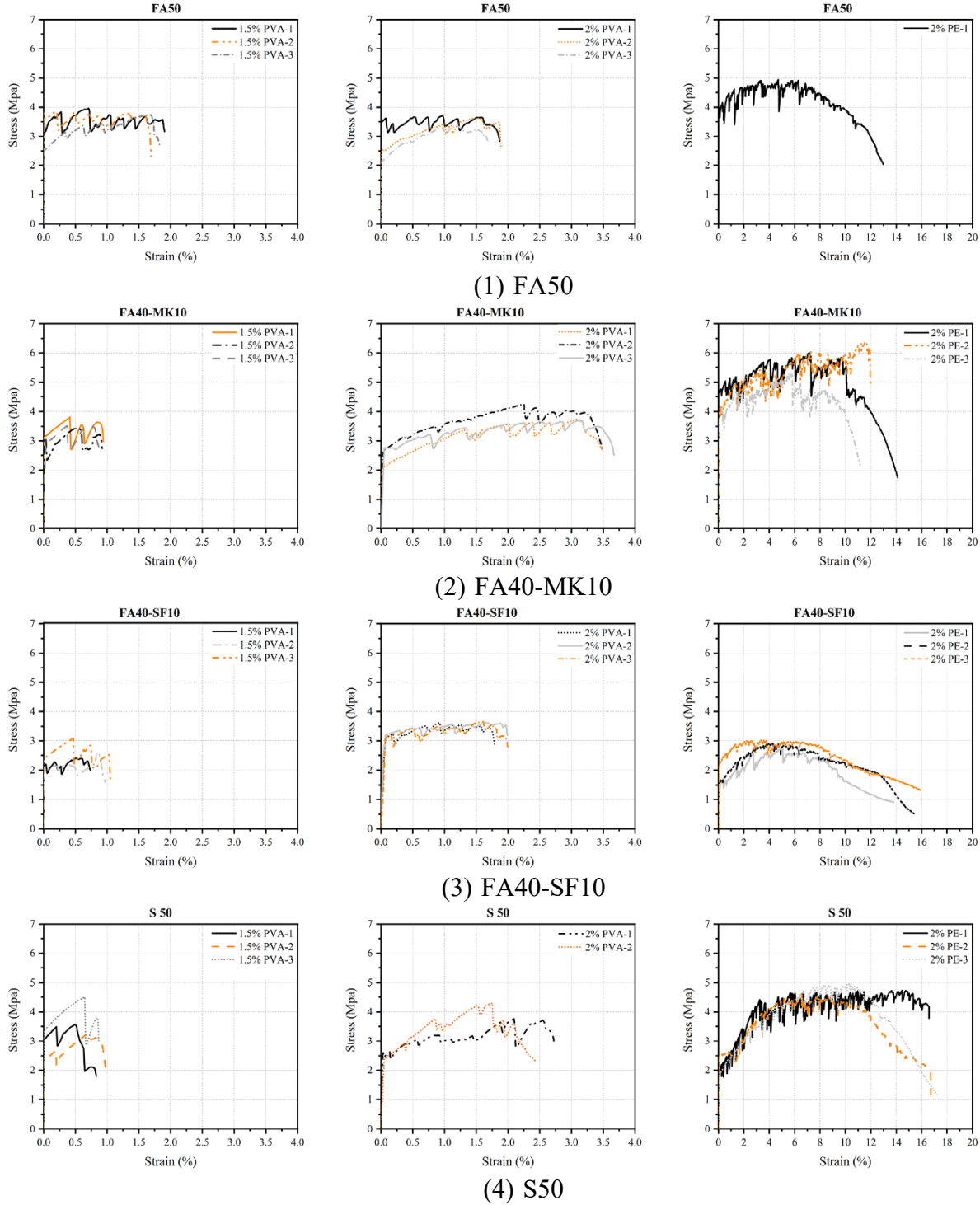


Figure 11. Direct tensile test strain and stress of different ECC mixes at 28-day age

Table 7. Tensile properties of ECC mixes after 28 days under uniaxial direct tensile test

Mix ID	Fibers content	First cracking stress (MPa)	Ultimate tensile strength (MPa)	Strain Capacity (%)	Toughness (MPa)
FA50	PVA 1.5	3.13 (± 0.50)	3.82 (± 0.10)	1.76 (± 0.11)	0.06 (± 0.01)
	PVA 2	2.71 (± 0.59)	3.51 (± 0.13)	1.78 (± 0.09)	0.06 (± 0.01)
	PE 2	3.66 (± 0.00)	4.91 (± 0.00)	11.27 (± 0.00)	0.52 (± 0.00)
FA40-MK10	PVA 1.5	2.93 (± 0.13)	3.76 (± 0.15)	0.86 (± 0.04)	0.03 (± 0.00)
	PVA 2	2.39 (± 0.24)	3.88 (± 0.26)	3.59 (± 0.23)	0.12 (± 0.01)
	PE 2	3.99 (± 0.43)	5.85 (± 0.42)	11.21 (± 0.9)	0.61 (± 0.08)
FA40-SF10	PVA 1.5	2.05 (± 0.14)	2.62 (± 0.36)	1.02 (± 0.05)	0.02 (± 0.00)
	PVA 2	3.17 (± 0.08)	3.61 (± 0.04)	1.87 (± 0.13)	0.07 (± 0.01)
	PE 2	1.76 (± 0.46)	2.95 (± 0.28)	12.09 (± 1.02)	0.31 (± 0.04)
S50	PVA 1.5	2.95 (± 0.45)	3.77 (± 0.54)	0.83 (± 0.04)	0.03 (± 0.01)
	PVA 2	2.59 (± 0.10)	4.03 (± 0.27)	2.4 (± 0.30)	0.09 (± 0.02)
	PE 2	2.16 (± 0.31)	4.73 (± 0.15)	15.88 (± 1.06)	0.60 (± 0.09)

*Note: the values in parentheses indicate the standard deviation of three measurements

4.4.3. Flexural Test

The flexural test results of load-displacement for all ECC 3D printed beams at 28-day are shown in Figure 13. For each mix, three tests were conducted to check the reliability of the measurement. These plots present the role of ECC mix design, the PVA fiber content (i.e., 1.5% vs. 2%), and fiber types (i.e., PVA vs. PE) on the flexural behavior of 3D-printed beams. Table 9 displays the moment capacity of each beam and the observed crack pattern. The moment capacity of each beam was calculated according to the following equation (Eq.1), developed for a 3-point bending test of a simply supported beam with a point load at the mid-span of the beam:

$$M_n = \frac{PL}{4} \quad (\text{Eq. 1})$$

where: M_n = moment capacity (KN.m)

P = load at the fracture point (KN)

L = length between supports (m)

Table 9 illustrates the moment capacity and deflection of all ECC samples. S50 had better moment capacity in different fiber contents among the four primary mix designs. For example, for 2% PVA and 2%PE fiber, the flexural moment capacity of S50 is 4% and 20% higher than FA50, respectively. In comparison, the deflection of FA50 specimens was 18% larger than that of S50. Substituting 10% of MK with FA in FA50 resulted in a nearly similar moment capacity, as reported in Table 8 while replacing FA with SF led to lower moment capacity (e.g., for 2%PE fiber ECC, FA50 has a 75% higher moment capacity compared to FA40-MK10). Furthermore, regarding deflection for 2%PE fiber, FA50 exhibited similar deflection to FA40-MK10, and 18% and 7% higher deflection compared to S50 and FA40-SF10, respectively.

Increasing the PVA fiber contents from 1.5% to 2% improves all ECC specimens' moment capacity and deflection, except FA50, as shown in Table 8. FA40-MK10 and FA40-SF10 demonstrated the most considerable improvement in moment capacity by 21% and 23%, respectively. In addition, FA50 containing 2% PE fibers exhibits a 40% higher moment capacity than the corresponding 2% PVA mix. For the FA40-SF10 mix, despite the improvement in deflection by altering the fiber from 2%PVA to 2%PE, the moment capacity decreased by 33%. This result is in good agreement with the values obtained from flexural strength.

The deflection of ECC samples containing PVA fibers is between 1-2 mm, whereas the corresponding deflection of specimens containing PE fibers is between 8-10 mm. The ECC with

1.5% and 2% PVA fibers exhibit none or negligible pseudo-strain hardening characteristics. On the other hand, 2%PE ECC samples indeed exhibit pseudo-strain hardening behavior under flexural load. Figure 12 illustrates the ultimate load against the incorporated mid-span deflection of all samples. In figure 11, there are two clusters of ECCs concerning strain capacity, a large group of PVA samples are in a less than 2% deflection area, and the other group is PE samples with a high deflection and ultimate load accumulated in a different area.

The considerable gap between the deflection of PE and PVA samples can be attributed to the physical difference in utilized fibers. It should be noted that the fiber failure mode and fiber status can significantly affect the strain capacity of ECC. When they carried stress exceeds the fiber strength, the rupture occurs, whereas pulled out occurs when the short side of fibers is pulled out of the matrix. One parameter that significantly affects the fiber's failure mode is fiber length. As the fiber length increases, the embedded length of fibers inside the matrix increases, resulting in a larger interfacial frictional force acting on the fibers. In other words, the increase in the length of fibers leads to higher interfacial friction between the fibers and matrix and ultimately results in a higher percentage of ruptured fibers [32].

As explained before, the diameter of PVA fibers is around 38 microns, whereas the diameter of PE fibers is around 15 microns. Indicating that in an equal weight of fibers, the PE fibers will have two times more surface area than PVA fibers to interact with the matrix, and ultimately the interfacial friction between the fibers and matrix will be two times higher than PVA fibers with a controlled crack width opening. Among the PE-reinforced specimens, the FA40-SF10-2%PE had a different behavior in terms of ultimate load. Nevertheless, the results are in agreement with the flexural test outcomes of an identical mix and confirm the integrity of conducted experiments.

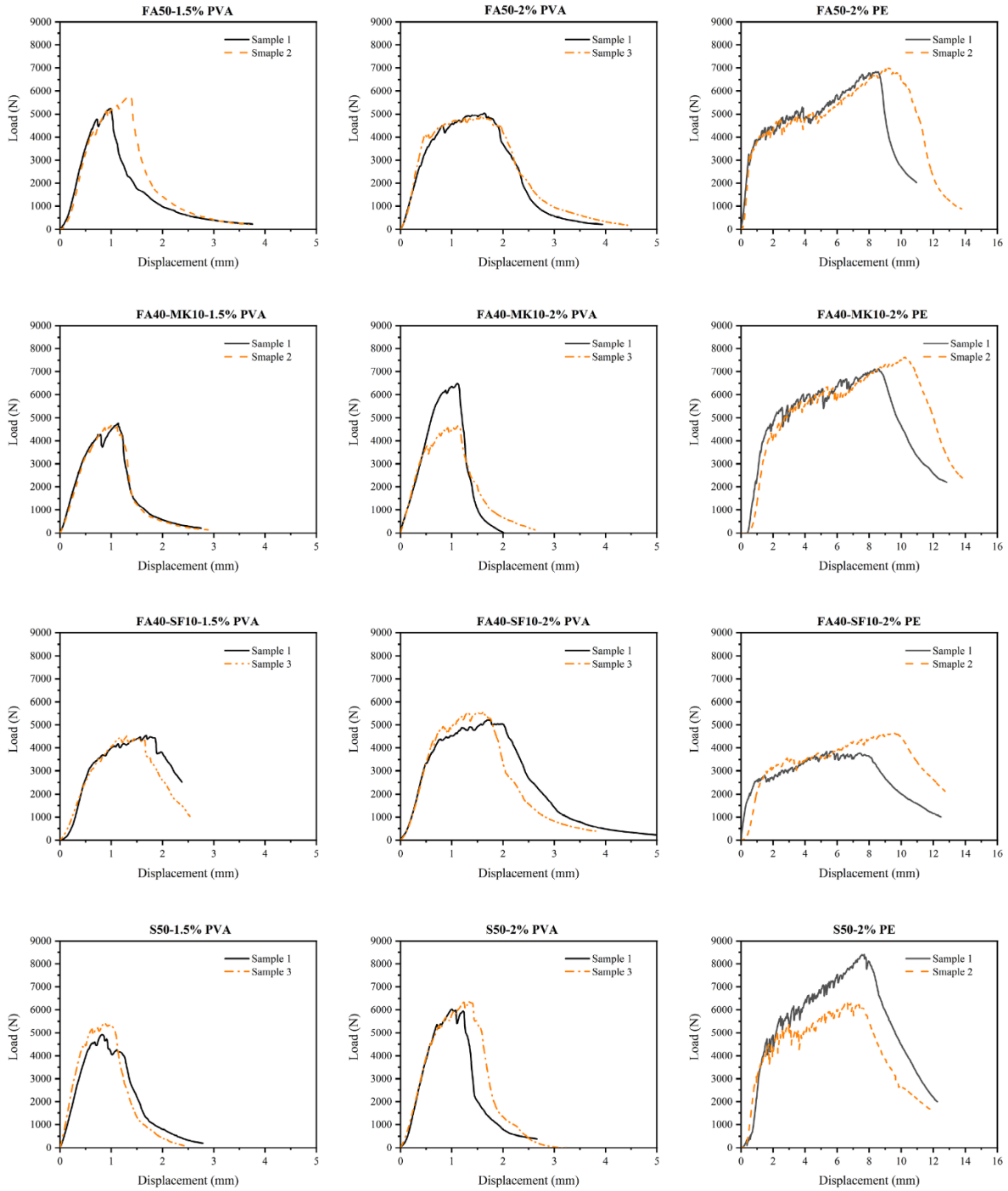




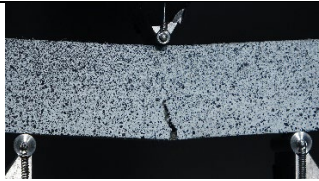









Figure 12. Load-Displacement of ECC printed beams containing 1.5% PVA, 2% PVA and 2%PE at 28 days of age.

Table 8. Results of flexural tests and failure patterns for different ECC mixes

Mix ID	Fiber's content	$M_{n \text{ ave}}$ (KN.m)	Deflection _{ave} (mm)	Failure Pattern
FA50	PVA 1.5	0.16	1.17 (± 0.20)	
	PVA 2	0.15	1.66 (± 0.03)	
	PE 2	0.21	8.87 (± 0.42)	
FA40-MK10	PVA 1.5	0.14	1.10 (± 0.01)	
	PVA 2	0.17	1.14 (± 0.02)	
	PE 2	0.22	9.48 (± 0.76)	
FA40-SF10	PVA 1.5	0.13	1.6 (± 0.17)	

	PVA 2	0.16	1.74 (± 0.18)	
	PE 2	0.12	8.84 (± 0.86)	
S50	PVA 1.5	0.15	0.87 (± 0.08)	
	PVA 2	0.18	1.17 (± 0.16)	
	PE 2	0.22	7.51 (± 0.17)	

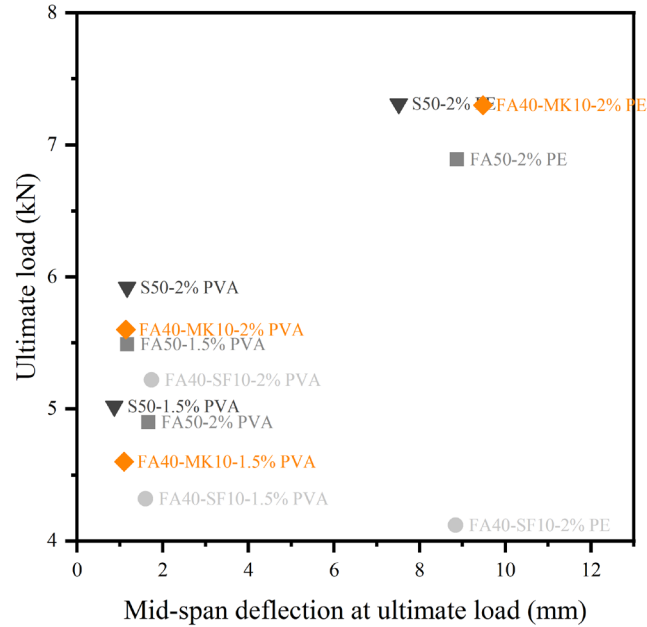


Figure 13. Relation between ultimate load and Mid-span deflection of ECC

4.5. Conclusions

This paper investigated the mechanical properties of four ECC mixes designed in our study's previous phase, and their fresh properties were all adjusted for 3D printing. In all of ECC mixes, 50% weight of OPC was replaced with FA, S, or combinations of 40FA and 10 MK and 40FA and 10SF. This study evaluated two types of fibers, including PVA and PE fibers. The PVA fiber content was assessed in two levels of 1.5% and 2% volume of the total mix. The mechanical properties of 3D-printed specimens were evaluated for compressive strength, tensile strength, and flexural strength. According to the finding of this paper, the following conclusions can be drawn:

- The compressive strength of 3D-printed cubes was lower than the cast ones. For example, for ECCs containing 1.5% PVA fibers, the compressive strength of the cast specimens was in the 53.5-59.0 MPa range, while for the 3D-printed cubes, this strength range dropped to 35.15-50.0 MPa.
- FA50-1.5PVA exhibited the max compressive strength reduction of 36% for cast vs. 3D-printed specimens. This compressive strength reduction could be attributed to forming voids between extruded filaments.
- The lower compressive strength was associated with the FA-rich mixes (i.e., FA50, FA40-MK10, and FA40-SF10), while S50 showed the maximum compressive strength in all 1.5%PVA and 2% of PVA and PE fibers cases.
- Replacing FA with MK or SF led to larger compressive strength and, at 2%PVA, improved the compressive strength of FA50 by 10% and 14% for FA40-MK10 and FA40-SF10, respectively.
- Increasing the PVA fiber quantity from 1.5% to 2% improves the compressive strength of ECC in all cases except FA50, which was reduced by 10%.
- For S50, the compressive strength of 3D-printed cubes was enhanced by 60 % by increasing PVA fiber from 1.5% to 2% and showed maximum strength improvement by adding more fibers.
- Replacing PVA with PE in mixes containing 2% fiber reduces compressive strength in all cases.

- The results from the compressive strength test prove that a higher compressive strength with a higher fiber content is achievable by adopting appropriate approaches to improve fiber distribution.
- The stress-strain results of different ECC mixes indicate the higher ductility of S50 compared to other mixes. For 2%PVA and 2%PE fiber, the strain capacity of S50 is 1.34 and 1.4times larger than F50, respectively.
- Substituting 10% of MK with FA in FA50 resulted in almost similar ultimate tensile strength, as reported in Table 7, while replacing FA with SF led to lower tensile strength.
- Increasing the PVA fiber contents from 1.5% to 2% enhances the strain capacity of all ECC mixes.
- Replacing the PVA fiber types with PE improved the toughness of all mixes around six times except FA40-SF10. The lower performance of FA40-SF10 in toughness can be attributed to the low first cracking strength of SF-rich mixtures.
- S50 had better moment capacity in different fiber contents among the four primary mix designs.
- In comparison, the deflection of FA50 specimens was 18% larger than that of S50. Substituting 10% of MK with FA in FA50 resulted in a nearly similar moment capacity, while replacing FA with SF led to a lower moment capacity.
- Increasing the PVA fiber contents from 1.5% to 2% improves all ECC specimens' moment capacity and deflection, except FA50.

- The considerable gap between the deflection of PE and PVA samples can be attributed to the physical difference in utilized fibers and interfacial frictional force acting on the fibers.
- All specimens containing PE fibers exhibited a high ductility and can be regarded as ultra-high ductile ECC with strain capacity over 10%.
- Regarding the fiber length, ECCs with 8mm PVA fibers could not achieve the desired strain capacity, whereas ECCs with 8mm PE fibers could surpass anticipations and achieve a strain capacity of over 10%.
- In this paper, some of the mixes, such as the S50-2%PE, demonstrated superior performance with 15.8% strain capacity and S50-2%PVA with 82.47 MPa compressive strength. According to this paper, it is possible to design an improved ECC with ultra-high ductile characteristics with locally available materials.

4.6. References:

- [1] L. Chong, S. Ramakrishna, and S. Singh, "A review of digital manufacturing-based hybrid additive manufacturing processes," *Int. J. Adv. Manuf. Technol.*, vol. 95, no. 5, pp. 2281–2300, 2018, doi: 10.1007/s00170-017-1345-3.
- [2] S. Wilkinson and N. Cope, "3D Printing and Sustainable Product Development," in *Green Information Technology: A Sustainable Approach*, Morgan Kaufmann, 2015, pp. 161–183.
- [3] A. Haleem and M. Javaid, "3D printed medical parts with different materials using additive manufacturing," *Clin. Epidemiol. Glob. Heal.*, vol. 8, no. 1, pp. 215–223, 2020, doi: 10.1016/j.cegh.2019.08.002.
- [4] V. Mohanavel, K. S. Ashraff Ali, K. Ranganathan, J. Allen Jeffrey, M. M. Ravikumar, and S. Rajkumar, "The roles and applications of additive manufacturing in the aerospace and

- automobile sector,” *Mater. Today Proc.*, vol. 47, pp. 405–409, 2021, doi: 10.1016/j.matpr.2021.04.596.
- [5] A. Paolini, S. Kollmannsberger, and E. Rank, “Additive manufacturing in construction: A review on processes, applications, and digital planning methods,” *Addit. Manuf.*, vol. 30, no. October, p. 100894, 2019, doi: 10.1016/j.addma.2019.100894.
- [6] J. Pegna, “Exploratory investigation of solid freeform construction,” *Autom. Constr.*, vol. 5, no. 5, pp. 427–437, 1997, doi: 10.1016/S0926-5805(96)00166-5.
- [7] V. C. Li *et al.*, “On the emergence of 3D printable Engineered, Strain Hardening Cementitious Composites (ECC/SHCC),” *Cem. Concr. Res.*, vol. 132, no. January, p. 106038, 2020, doi: 10.1016/j.cemconres.2020.106038.
- [8] G. H. Ahmed, N. H. Askandar, and G. B. Jumaa, “A review of largescale 3DCP : Material characteristics , mix design , printing process , and reinforcement strategies,” *Structures*, vol. 43, no. July, pp. 508–532, 2022, doi: 10.1016/j.istruc.2022.06.068.
- [9] M. Hojati, Z. Li, A. M. Memari, K. Park, M. Zahabi, and S. Nazarian, “3D-printable quaternary cementitious materials towards sustainable development : Mixture design and mechanical properties,” vol. 13, no. January, 2022, doi: 10.1016/j.rineng.2022.100341.
- [10] A. Bakhshi, R. Sedghi, and M. Hojati, “A Preliminary Study on the Mix Design of 3D-Printable Engineered Cementitious Composite,” in *Tran-SET 2021*, 2021, pp. 199–211.
- [11] M. Zafar, MS, Bakhshi, A., Hojati, “Towards 3D-printable engineered cementitious composites: mix design proportioning, flowability, and mechanical performance,” 2022.
- [12] M. Zafar, MS, Bakhshi, A., Hojati, “Evaluating the printing quality of 3D-printable

- engineered cementitious composites by utilizing viscosity modifying admixture,” *Addit. Manuf.*, 2023.
- [13] V. C. Li *et al.*, “On the emergence of 3D printable Engineered, Strain Hardening Cementitious Composites (ECC/SHCC),” *Cem. Concr. Res.*, vol. 132, no. April, p. 106038, 2020, doi: 10.1016/j.cemconres.2020.106038.
- [14] D. G. Soltan and V. C. Li, “A self-reinforced cementitious composite for building-scale 3D printing,” *Cem. Concr. Compos.*, vol. 90, pp. 1–13, 2018, doi: 10.1016/j.cemconcomp.2018.03.017.
- [15] K. Yu, L. Li, J. Yu, J. Xiao, J. Ye, and Y. Wang, “Feasibility of using ultra-high ductility cementitious composites for concrete structures without steel rebar,” *Eng. Struct.*, vol. 170, no. May, pp. 11–20, 2018, doi: 10.1016/j.engstruct.2018.05.037.
- [16] B. Zhu, J. Pan, Z. Zhou, and J. Cai, “Mechanical properties of engineered cementitious composites beams fabricated by extrusion-based 3D printing,” *Eng. Struct.*, vol. 238, no. October 2020, p. 112201, 2021, doi: 10.1016/j.engstruct.2021.112201.
- [17] K. Yu, W. McGee, T. Y. Ng, H. Zhu, and V. C. Li, “3D-printable engineered cementitious composites (3DP-ECC): Fresh and hardened properties,” *Cem. Concr. Res.*, vol. 143, no. September 2020, 2021, doi: 10.1016/j.cemconres.2021.106388.
- [18] A. E. Naaman and H. W. Reinhardt, “Proposed classification of HPFRC composites based on their tensile response,” *Mater. Struct.*, vol. 39, no. 5, pp. 547–555, 2006, doi: 10.1617/s11527-006-9103-2.
- [19] E. H. Yang, S. Wang, Y. Yang, and V. C. Li, “Fiber-bridging constitutive law of engineered

- cementitious composites,” *J. Adv. Concr. Technol.*, vol. 6, no. 1, pp. 181–193, 2008, doi: 10.3151/jact.6.181.
- [20] J. Zhang and B. Leng, “Transition from Multiple Macro-Cracking to Multiple Micro-Cracking in Cementitious Composites,” *Tsinghua Sci. Technol.*, vol. 13, no. 5, pp. 669–673, 2008, doi: 10.1016/S1007-0214(08)70109-3.
- [21] V. C. Li, D. K. Mishra, and H. C. Wu, “Matrix design for pseudo-strain-hardening fibre reinforced cementitious composites,” *Mater. Struct.*, vol. 28, pp. 586–595, 1995.
- [22] A. A. A. Hassan, M. Lachemi, and K. M. A. Hossain, “Effect of metakaolin and silica fume on the durability of self-consolidating concrete,” *Cem. Concr. Compos.*, vol. 34, no. 6, pp. 801–807, Jul. 2012, doi: 10.1016/j.cemconcomp.2012.02.013.
- [23] M. D. A. Thomas, “Optimizing the Use of Fly Ash in Concrete,” *Portl. Cem. Assoc.*, p. 24, 2007.
- [24] H. Noorvand, G. Arce, M. M. Hassan, and T. Rupnow, “Performance of engineered cementitious composites utilizing locally available materials in the state of Louisiana,” *Proceedings, Annu. Conf. - Can. Soc. Civ. Eng.*, vol. 2019-June, no. Mai 1995, pp. 1–10, 2019.
- [25] Y. Zhu, Y. Yang, and Y. Yao, “Use of slag to improve mechanical properties of engineered cementitious composites (ECCs) with high volumes of fly ash,” *Constr. Build. Mater.*, vol. 36, pp. 1076–1081, 2012, doi: 10.1016/j.conbuildmat.2012.04.031.
- [26] E. H. Yang, Y. Yang, and V. C. Li, “Use of high volumes of fly ash to improve ECC mechanical properties and material greenness,” *ACI Mater. J.*, vol. 104, no. 6, pp. 620–628,

- 2007, doi: 10.14359/18966.
- [27] D. N. Richardson, “Strength and Durability Characteristics of a 70% Ground Granulated Blast Furnace Slag (GGBFS) Concrete Mix,” vol. 2006, p. 94, 2006, [Online]. Available: <http://library.modot.mo.gov/RDT/reports/Ri99035/or06008.pdf>.
- [28] P. Norrarat, W. Tangchirapat, S. Songpiriyakij, and C. Jaturapitakkul, “Evaluation of Strengths from Cement Hydration and Slag Reaction of Mortars Containing High Volume of Ground River Sand and GGBF Slag,” *Adv. Civ. Eng.*, vol. 2019, 2019, doi: 10.1155/2019/4892015.
- [29] Y. Li, X. Guan, C. Zhang, and T. Liu, “Development of High-Strength and High-Ductility ECC with Saturated Multiple Cracking Based on the Flaw Effect of Coarse River Sand,” *J. Mater. Civ. Eng.*, vol. 32, no. 11, pp. 1–11, 2020, doi: 10.1061/(asce)mt.1943-5533.0003405.
- [30] B. Zhu, J. Pan, B. Nematollahi, Z. Zhou, Y. Zhang, and J. Sanjayan, “Development of 3D printable engineered cementitious composites with ultra-high tensile ductility for digital construction,” *Mater. Des.*, vol. 181, no. July, p. 108088, 2019, doi: 10.1016/j.matdes.2019.108088.
- [31] W. Zhou, Y. Zhang, L. Ma, and V. C. Li, “Influence of printing parameters on 3D printing engineered cementitious composites (3DP-ECC),” *Cem. Concr. Compos.*, vol. 130, no. January, p. 104562, 2022, doi: 10.1016/j.cemconcomp.2022.104562.
- [32] B. T. Huang, J. Q. Wu, J. Yu, J. G. Dai, C. K. Y. Leung, and V. C. Li, “Seawater sea-sand engineered/strain-hardening cementitious composites (ECC/SHCC): Assessment and modeling of crack characteristics,” *Cem. Concr. Res.*, vol. 140, no. November 2020, p.

- 106292, 2021, doi: 10.1016/j.cemconres.2020.106292.
- [33] J. Zhou, S. Qian, G. Ye, O. Copuroglu, K. Van Breugel, and V. C. Li, “Improved fiber distribution and mechanical properties of engineered cementitious composites by adjusting the mixing sequence,” *Cem. Concr. Compos.*, vol. 34, no. 3, pp. 342–348, 2012, doi: 10.1016/j.cemconcomp.2011.11.019.
- [34] Japan Society of Civil Engineers, “Recommendations for Design and Construction of High Performance Fiber Reinforced Cement Composites with Multiple Fine Cracks (HPFRCC),” *Concr. Eng. Ser.*, vol. 82, p. Testing Method 6-10, 2008, [Online]. Available: <http://www.jsce.or.jp/committee/concrete/e/index.html>.
- [35] Z. Li *et al.*, “Fresh and hardened properties of extrusion-based 3D-printed cementitious materials: A review,” *Sustain.*, vol. 12, no. 14, pp. 1–33, 2020, doi: 10.3390/su12145628.
- [36] T. T. Le *et al.*, “Hardened properties of high-performance printing concrete,” *Cem. Concr. Res.*, vol. 42, no. 3, pp. 558–566, 2012, doi: 10.1016/j.cemconres.2011.12.003.
- [37] Z. Duan, L. Li, Q. Yao, S. Zou, A. Singh, and H. Yang, “Effect of metakaolin on the fresh and hardened properties of 3D printed cementitious composite,” *Constr. Build. Mater.*, vol. 350, no. August, p. 128808, 2022, doi: 10.1016/j.conbuildmat.2022.128808.
- [38] Z. Pan, C. Wu, J. Liu, W. Wang, and J. Liu, “Study on mechanical properties of cost-effective polyvinyl alcohol engineered cementitious composites (PVA-ECC),” *Constr. Build. Mater.*, vol. 78, pp. 397–404, 2015, doi: 10.1016/j.conbuildmat.2014.12.071.
- [39] S. H. Said, H. A. Razak, and I. Othman, “Flexural behavior of engineered cementitious composite (ECC) slabs with polyvinyl alcohol fibers,” *Constr. Build. Mater.*, vol. 75, pp.

- 176–188, 2015, doi: 10.1016/j.conbuildmat.2014.10.036.
- [40] Z. Cheng *et al.*, “Effect of fiber content on the mechanical properties of engineered cementitious composites with recycled fine aggregate from clay brick,” *Materials (Basel)*., vol. 14, no. 12, 2021, doi: 10.3390/ma14123272.
- [41] J. K. Kim, J. S. Kim, G. J. Ha, and Y. Y. Kim, “Tensile and fiber dispersion performance of ECC (engineered cementitious composites) produced with ground granulated blast furnace slag,” *Cem. Concr. Res.*, vol. 37, no. 7, pp. 1096–1105, 2007, doi: 10.1016/j.cemconres.2007.04.006.
- [42] S. H. Said and H. A. Razak, “The effect of synthetic polyethylene fiber on the strain hardening behavior of engineered cementitious composite (ECC),” *Mater. Des.*, vol. 86, pp. 447–457, 2015, doi: 10.1016/j.matdes.2015.07.125.

Chapter 5

5. Conclusion and Future work

5.1. Conclusion

With current developments in conventional reinforcement methods (e.g., rebar reinforcement) using manual techniques, the concept of fully automated 3D concrete printing (3DCP) construction with minimum human contact cannot be realized. To overcome these problems, this research proposed incorporating a high volume of fibers and achieving superior mechanical properties for the designed printable mixes. The feasibility of using Engineered cementitious composite (ECC), as a Strain Hardening Cement-based material or bendable concrete, was investigated in detail.

This research aimed to design a printable ECC mix design with superior mechanical performance and high ductility to diminish the demand for rebar reinforcements for 3DPC applications in the construction industry. According to experimental results from the fresh and hardened properties of ECC samples, it can be concluded that designing a 3D printed ECC with bendable and ductile performance is achievable. Accordingly, several ECC mixtures were developed with superior printability and ultra-high ductility (over 8% strain capacity) for 3DCP applications.

The mechanical performance of developed 3D printable ECC mixtures was far beyond expectations and can be considered one of the most ductile ECC suitable for 3D printing to date.

While using primary methods such as flow table test and setting time lack the accuracy of other equipment, this approach provides a general insight into the fresh properties of mixtures.

According to the acquired test results, the following conclusions can be drawn:

1. The workability of fresh ECC mixtures was improved using fly ash. It led to a lower W/B ratio of fly ash-rich ECC (i.e., FA50 and FA75), while the slag-rich ECC mixtures (i.e., S50 and S75) demanded more water to reach the desired flowability.
2. The inclusion of fly ash in ECC improved the fiber dispersion and enhanced the fresh properties of fresh mixtures. However, spherical fly ash particles sliding in fly ash-rich mixtures (such as FA75) would lower the material's interlocking and load transition capability and mechanical performance, as observed for FA75 compared to FA50.
3. The compressive strength of mixtures with 50% substitution of cement by slag or fly ash led to a higher compressive strength than the 75% replacement level, indicating the influential role of cement on ECC mixtures strength development.
4. The compressive strength of 3D-printed cubes was lower than the cast ones due to the forming void between the printed filaments in the printing process. FA50-1.5PVA exhibited the max compressive strength reduction of 36% for cast vs. 3D-printed specimens. The compressive strength of the cast specimens was in the 53.5-59.0 MPa range, while for the 3D-printed cubes, this strength range dropped to 35.15-50.0 MPa.
5. While S50 exhibited the maximum compressive strength in all 1.5%PVA and 2% of PVA and PE fibers cases, the FA-rich mixes (i.e., FA50, FA40-MK10, and FA40-SF10) had the lower compressive strength.
6. Substituting FA with SF and MK led to higher compressive strength and, at 2%PVA, improved the compressive strength of FA50 by 10% and 14% for FA40-MK10 and FA40-SF10, respectively.
7. The results demonstrated that increasing the PVA fiber quantity from 1.5% to 2% improves the compressive strength of ECC in all cases except FA50, which was reduced by 10%.

8. The compressive strength of S50 was enhanced by 60% by increasing PVA fiber from 1.5% to 2% and showed maximum strength improvement by adding more fibers.
9. Replacing PVA with PE in ECCs containing 2% fibers lowers the compressive strength in all cases.
10. The higher compressive strength with increasing fiber contents is achievable by adopting appropriate approaches to improve fiber distribution.
11. S50 had better moment capacity in different fiber contents among the four primary mix designs.
12. Replacing 10% of FA in FA50 with MK resulted in almost similar ultimate tensile strength while replacing FA with SF led to lower tensile strength.
13. Increasing the PVA fiber contents from 1.5% to 2% enhances the strain capacity of all ECC mixes.
14. The toughness of all ECC specimens was improved around six times by replacing the PVA fiber types with PE fibers.
15. In comparison, the deflection of FA50 specimens was 18% higher than that of S50. Replacing 10% of FA in FA50 with MK resulted in a nearly similar moment capacity, while replacing FA with SF led to a lower moment capacity.
16. Increasing the PVA fiber contents from 1.5% to 2% improves all ECC specimens' moment capacity and deflection, except FA50.
17. The considerable gap between the deflection of PE and PVA samples can be attributed to the physical difference in utilized fibers and interfacial frictional force acting on the fibers.
18. The considerable gap between the deflection of PE and PVA samples in the flexural test can be caused by an interfacial frictional force acting on the fibers originating from the

difference in the physical properties of utilized fibers. All specimens containing a 2% volume fraction of PE fibers exhibited a high ductility (over 10% strain capacity) and can be considered ultra-high ductile ECC.

19. The mixes containing PVA fiber could not achieve the desired strain capacity (i.e., less than 2% strain capacity) despite having a proper volume of PVA fibers (between 1%-2% volume fraction), whereas the PE samples exceeded 10% strain capacity.

5.2. Future work

To better understand the implications of developed ECC in actual 3D printed structures, future studies could address the feasibility of using ECC on a large scale by evaluating the mechanical performance of printed beams and columns or testing a frame of the printed building. In addition, further research is needed to determine the relationship between fiber length and tensile performance of PVA fiber-reinforced ECC for printed samples.